

RESPONSE SURFACE BASED PERFORMANCE ANALYSIS OF AN
AIR-DEFENSE MISSILE SYSTEM

A THESIS SUBMITTED TO
THE GRADUATE SCHOOL OF NATURAL AND APPLIED SCIENCES
OF
MIDDLE EAST TECHNICAL UNIVERSITY

BY

KEREM GÜNAYDIN

IN PARTIAL FULLFILLMENT OF THE REQUIREMENTS
FOR
THE DEGREE OF MASTER OF SCIENCE
IN
AEROSPACE ENGINEERING

AUGUST 2014

Approval of the thesis:

**RESPONSE SURFACE BASED PERFORMANCE ANALYSIS OF AN
AIR-DEFENSE MISSILE SYSTEM**

submitted by **KEREM GÜNAYDIN** in partial fulfillment of the requirements for the degree of **Master of Science in Aerospace Engineering Department, Middle East Technical University** by,

Prof. Dr. Canan Özgen
Dean, Graduate School of **Natural and Applied Sciences**

Prof. Dr. Ozan Tekinalp
Head of Department, **Aerospace Engineering**

Prof. Dr. Ozan Tekinalp
Supervisor, **Aerospace Engineering Dept., METU**

Examining Committee Members

Assoc. Prof. Dr. Tayfun Çimen
Roketsan Missiles Industries Inc.

Prof. Dr. Ozan Tekinalp
Aerospace Engineering Dept., METU

Prof. Dr. Kemal Leblebicioğlu
Electrical and Electronical Engineering Dept., METU

Asst. Prof. Dr. Ali Türker Kutay
Aerospace Engineering Dept., METU

Assoc. Prof. Dr. İlkey Yavrucuk
Aerospace Engineering Dept., METU

Date: 27.08.2014

I hereby declare that all information in this document has been obtained and presented in accordance with academic rules and ethical conduct. I also declare that, as required by these rules and conduct, I have fully cited and referenced all material and results that are not original to this work.

Name, Last name : Kerem GÜNAYDIN

Signature :

ABSTRACT

RESPONSE SURFACE BASED PERFORMANCE ANALYSIS OF AN AIR-DEFENSE MISSILE SYSTEM

Günaydın, Kerem

M. S., Department of Aerospace Engineering

Supervisor: Prof. Dr. Ozan Tekinalp

August 2014, 67 pages

In this thesis, response surface based performance analysis of an air defense missile system was performed. System performance defined as the probability of hit is determined using a conventional grid analysis in order to set up a control group. Then, some experiments were designed to construct response surfaces (RSM). Simulation model was run for these experiment points. Response surfaces for the whole operational area of an air defense missile system is developed using these experiments, so as to be able to predict the system performance without running at every sample point for different types of target engagement scenarios. The PoH (Probability of Hit) graphics related to these scenarios were obtained and presented. Finally, the PoH graphics regarding to the RSM experimental designs were compared with the ones generated from GRID analysis.

Keywords: Design of Experiments, Response Surface Methodology, Performance Analysis, Missile Systems.

ÖZ

CEVAP YÜZEYİ YÖNTEMİ KULLANILARAK BİR HAVA SAVUNMA FÜZE SİSTEMİNİN PERFORMANS ANALİZİ

Günaydın, Kerem

Yüksek Lisans, Havacılık ve Uzay Mühendisliği Bölümü

Tez Yöneticisi : Prof. Dr. Ozan Tekinalp

Ağustos 2014, 67 sayfa

Bu tezde, tipik bir hava savunma füze sisteminin performans analizi yapılmıştır. Vuruş olasılığı değeri olarak tanımlanan system performansına dair elde edilen analiz sonuçlarını kıyaslayabilmek için geleneksel bir yöntem olan eşdeğer aralıklarına sahip ızgara(grid) yöntemi kullanılarak kontrol kümesi oluşturulmuştur. Kontrol kümesi ile ilgili analizler yapıldıktan sonra, cevap yüzeylerini elde edebilmek için bazı deneyler tasarlanmıştır. Buradaki deney kombinasyonlarına göre simülasyon koşturulmuştur. Bu sayede, farklı hedef angajman senaryoları dahilinde füze performansını incelemek için bütün noktalarda koşum atmaya gerek kalmaksızın cevap yüzeyleri oluşturulmuştur. Buradaki matematiksel modellere dayanarak füze sisteminin başarımını ölçmek adına vuruş olasılığı grafikleri çıkartılmış ve geleneksel yöntemle yapılan analizlerin sonuçlarıyla kıyaslanmıştır.

Anahtar kelimeler: Deneysel Tasarım, Cevap Yüzeyi Yöntemi, Performans Analizi, Füze Sistemleri

To my family

ACKNOWLEDGEMENTS

I would like to express my gratitude to my supervisor, Prof. Dr. Ozan Tekinalp, and my co-advisor and also colleague, Assoc. Dr. Tayfun Çimen, for their unlimited hours of expertise and guidance throughout my study. It would have been impossible for me to find my way through the complicated work, without their mentoring.

I am also thankful to my colleagues and my chief Ercan Örücü in ROKETSAN Missile Industries Inc. for their understanding and support.

I am grateful to my parents Melek and Muharrem, and also my brother Murat, for their endless love and support. They have always been there for me. I took their love and good wishes for granted, to be able to smile at all the pessimism I have faced in life.

I wish to express my sincere thanks to all my friends for the patience they have shown throughout my lengthy graduate program experience. I've always felt as a part of a much bigger family than my own.

For her kind and loving embracement, for her understanding, and for the inspiration she granted, I am grateful to my love, Gözde. If I hadn't have her understanding, I wouldn't have completed this study.

TABLE OF CONTENTS

ABSTRACT	v
ÖZ	vi
ACKNOWLEDGEMENTS	viii
TABLE OF CONTENTS	ix
LIST OF FIGURES	xi
LIST OF TABLES	xiv
NOMENCLATURE	xv
CHAPTERS	
1 INTRODUCTION	1
1.1 Theoretical Background.....	1
1.1.1 Performance Analysis.....	1
1.1.2 Motivation of the Thesis.....	3
1.1.3 Design of Experiments	4
1.1.4 Response Surface Method	9
1.2 Contribution of the Thesis	10
1.3 Scope of the Thesis	11
2 ADMS TOOL AND ENGAGEMENT SCENARIOS	13
2.1 ADMS Tool	13
2.2 Engagement Scenarios	17
3 GRID METHODOLOGY FOR PERFORMANCE ANALYSIS	21
3.1 Non-Maneuvering Scenarios	21
3.2 Maneuvering Scenarios.....	25
4 RESPONSE SURFACE METHODOLOGY BASED DESIGN OF EXPERIMENTS	31
4.1 Formulation of Response Surface Methodology	31

4.2	Response Surface Design Process.....	36
4.3	RSM Approach to Performance Analysis Problem	37
4.3.1	RSM Approach for Non-Maneuvering Case	38
4.3.2	RSM Approach for Maneuvering Cases	43
4.3.2.1	RSM Approach for Maneuvering Start-up Range %12.....	44
4.3.2.2	RSM Approach for Maneuvering Start-up Range %18.....	49
5	COMPARISON OF GRID AND RESPONSE SURFACE METHODS.....	55
5.1	Comparison for Non-Maneuvering Case	55
5.2	Comparison for Maneuvering Start-up Range %12.....	58
5.3	Comparison for Maneuvering Start-up Range %18.....	60
6	CONCLUSION.....	63
6.1	General Conclusions	63
6.2	Recommendations for Future Work.....	64
	REFERENCES.....	65

LIST OF FIGURES

FIGURES

Figure 1 Performance Analysis Cycle via Experimental Design	2
Figure 2 Balance btw Analysis Detail and Cost (Man Hour)	3
Figure 3 Elements and Components of an Experimental Design Process	7
Figure 4 Residual Plots Regarding to the Adequacy Check	8
Figure 5 Response Surface Method Process [28]	9
Figure 7 ADMS Tool	14
Figure 8 Performance Analysis Tree regarding to Predefined Inputs	15
Figure 9 Missile Operational Areas for the Non-Maneuvering Target Case	22
Figure 10 PoH Results for GRID approach for Non-Maneuvering Case at LOR %20	23
Figure 11 PoH Results for GRID approach for Non-Maneuvering Case at LOR %30	23
Figure 12 PoH Results for GRID approach for Non-Maneuvering Case at LOR %40	24
Figure 13 Missile Operational Areas for Maneuvering Cases	25
Figure 14 PoH Results for GRID approach for Maneuver Start-up Range %12 at LOR % 12	26
Figure 15 PoH Results for GRID approach for Maneuver Start-up Range %12 at LOR % 18	27
Figure 16 PoH Results for GRID approach for Maneuver Start-up Range %12 at LOR % 24	27
Figure 17 PoH Results for GRID approach for Maneuver Start-up Range %18 at LOR % 12	28
Figure 18 PoH Results for GRID approach for Maneuver Start-up Range %18 at LOR % 18	28
Figure 19 PoH Results for GRID approach for Maneuver Start-up Range %18 at LOR % 24	29

Figure 20 Sample Locations for Response Surface Construction: Central Composite (left) and Box-Behnken (right)	35
Figure 21 Response Surface Based Experimental Design Project Process Loop	36
Figure 22 Division of the operation area for RSM Construction.....	38
<i>Figure 23 Residual Plots for PoH for Non-Maneuvering Case regarding to first part</i>	40
<i>Figure 24 Residual Plots for PoH for Non-Maneuvering Case regarding to second part</i>	41
Figure 25 PoH Results for RSM approach for Non-Maneuvering Case at LOR %20	42
Figure 26 PoH Results for RSM approach for Non-Maneuvering Case at LOR %30	42
Figure 27 PoH Results for RSM approach for Non-Maneuvering Case at LOR %40	43
Figure 28 Residual Plots for PoH for Maneuver Start-up range %12 regarding to first part	46
Figure 29 Residual Plots for PoH for Maneuver Start-up range %12 regarding to second part	46
Figure 30 PoH Results for RSM approach for Maneuver Start-up Range %12 at LOR %20	47
Figure 31 PoH Results for RSM approach for Maneuver Start-up Range %12 at LOR %30	48
Figure 32 PoH Results for RSM approach for Maneuver Start-up Range %12 at LOR %40	48
<i>Figure 33 Residual Plots for PoH for Maneuver Start-up range %18 regarding to first part</i>	51
<i>Figure 34 Residual Plots for PoH for Maneuver Start-up range %18 regarding to second part</i>	51
Figure 35 PoH Results for RSM approach for Maneuver Start-up Range %18 at LOR %20	52
Figure 36 PoH Results for RSM approach for Maneuver Start-up Range %18 at LOR %30	53

Figure 37 PoH Results for RSM approach for Maneuver Start-up Range %18 at LOR %40	53
Figure 38 Comparison of PoH Results btw grid and RSM approaches for non-maneuver case LOR %40	55
Figure 39 Comparison of PoH Results btw grid and RSM approaches for non-maneuver case LOR %40	56
Figure 40 Comparison of PoH Results btw grid and RSM approaches for non-maneuver case LOR %40	56
Figure 41 Comparison of PoH Results btw grid and RSM approaches for maneuver start-up range %12 at LOR %12.....	58
Figure 42 Comparison of PoH Results btw grid and RSM approaches for maneuver start-up range %12 at LOR %18.....	59
Figure 43 Comparison of PoH Results btw grid and RSM approaches for maneuver start-up range %12 at LOR %24.....	59
Figure 44 Comparison of PoH Results btw grid and RSM approaches for maneuver start-up range %18 at LOR %12.....	60
Figure 45 Comparison of PoH Results btw grid and RSM approaches for maneuver start-up range %18 at LOR %18.....	61
Figure 46 Comparison of PoH Results btw grid and RSM approaches for maneuver start-up range %18 at LOR %24.....	61

LIST OF TABLES

TABLES

Table 1 Different Type of Fractional Factorial Designs	5
Table 2 Taguchi Design Table	6
Table 3 Table of Scenarios used in the Study	18
Table 4 First Part of the Domain with CCD for Non-Maneuvering Case	38
Table 5 Second Part of the Domain with CCD for Non-Maneuvering Case	39
Table 6 First Part of the Domain with CCD for Maneuvering Startup Range %12 ..	44
Table 7 Second Part of the Domain with CCD for Maneuvering Startup Range %12	44
Table 8 First Part of the Domain with CCD for Maneuvering Startup Range %18 ..	49
Table 9 Second Part of the Domain with CCD for Maneuvering Startup Range %18	49

NOMENCLATURE

SYMBOLS

y	Response
x	Parameters
β	Coefficients
ϵ	Errors
L	Least Square Estimator
SS	Sum of Squares
E	Estimation

SUPERSCRIPTS

$'$	Transpose of Matrix
-----	---------------------

SUBSCRIPTS

ij	Element of Matrix at i 'th Row and j 'th Column
------	---

CHAPTER 1

INTRODUCTION

1.1 Theoretical Background

1.1.1 Performance Analysis

Performance analysis studies can be considered in many ways from the simplest system to the most complex system combinations. The motivation for these studies is generally to see if the whole system performance satisfies the requirements or not.

For analyzing it, there is a long way from the system to the subsystem levels step by step. At every step, subsystems are tested regarding to the requirements in order to generate a successful system. The idea behind these steps is to minimize the errors and uncertainties, so every step has to be examined in detail. This process also provides an opportunity for designer and/or analyzer to see the influences of every subsystem over the whole system performance and compare each other [1]. A simple process for system performance analysis cycle related to the subsystems, or in another way factors, can be shown in Figure 1:

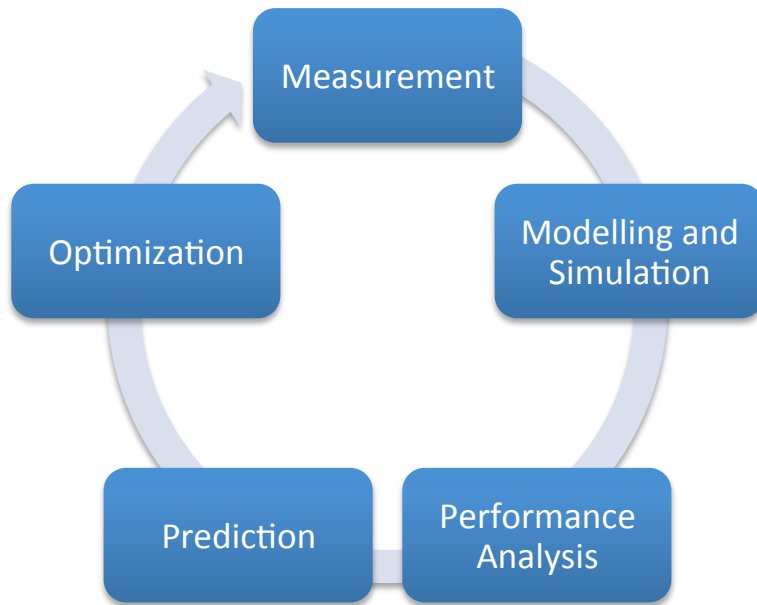


Figure 1 Performance Analysis Cycle via Experimental Design

It can be seen that the general performance analysis cycle is consisted of four steps. First two steps named as “Measurement and Modeling & Simulation” come before the performance analysis process. Initially, measurements are done for the related experiments. After that, convenient model is constructed and simulations are run according to the requirements. After obtaining the results from simulations, performance analysis process is carried out [1,2].

In general performance analysis has 4 phases. First phase is the determination of the factors and the test conditions. Second one is for constructing the experimental methods. Analysis is the third phase. Finally in the fourth phase, the validation of the experiments comes [1,2].

For missile systems, the top-level requirement is generally the Probability of Hit (PoH). Every study is based on the idea of maximizing the PoH value. Both the physical aspects and algorithmic studies are focused on this objective.

After performance analysis process, prediction phase comes. In this phase, future possibilities about the results are predicted. Finally, the factors are optimized regarding to the performance requirements with the help of results obtained from simulations and predictions.

1.1.2 Motivation of the Thesis

The performance of an Air Defense Missile System (ADMS), namely the probability of hit (PoH) performance, is evaluated using full grid analysis approach and response surface approach and these two approaches are compared. For this purpose, a detailed six degrees of freedom missile simulation model is employed. The parameters are varied with prescribed uncertainties for performing Monte-Carlo runs in order to estimate the PoH of a hypothetical missile. Because such high-fidelity models are necessary for performance analysis, the analysis process is usually very time consuming and computationally expensive. Moreover, engagement scenarios directly depend on target capabilities. Such capabilities enforce the analyst to run more simulations to obtain accurate results under various error and uncertainty conditions [3,4].

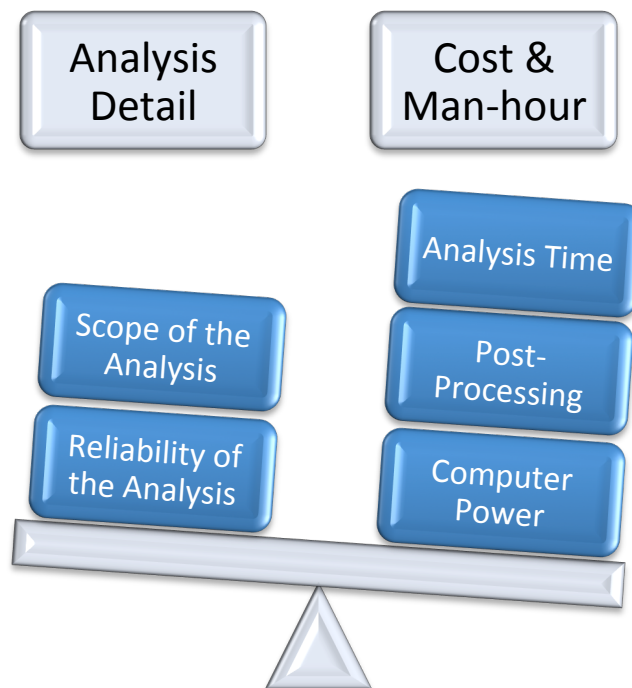


Figure 2 Balance btw Analysis Detail and Cost (Man Hour)

In this study, a response surface method is employed using fundamental parameters that affect the PoH. Engagement downrange and altitude, and seeker lock-on-range of the missile are selected as the fundamental inputs. Sampling points related to conventional grid and response surfaces in the experimental design are analyzed by

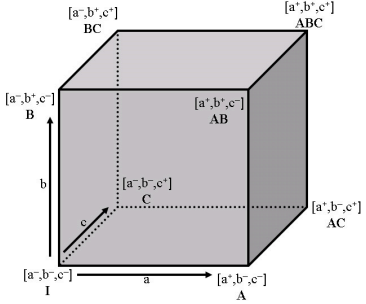
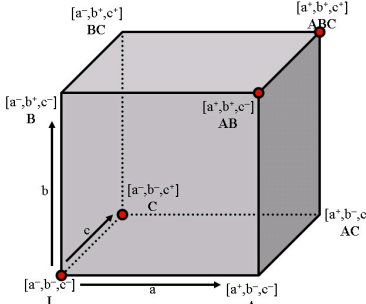
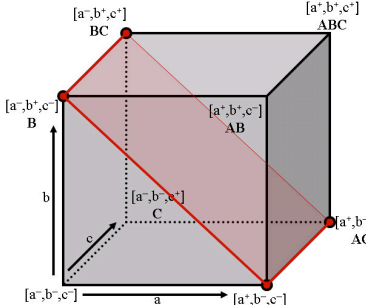
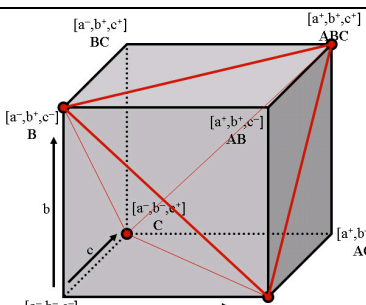
the ADMS modeling and simulation tool. The concepts, techniques and practical applications of Design of Experiments (DoE) methods are investigated for ADMS to obtain the non-maneuvering and also the optimum target evasive maneuvering situation. The number of simulations required to determine the performance of ADMS against different maneuvering target is analyzed for minimizing the required number of runs. And for the maneuvering targets, it is assumed to have full information about the pursuing missile as a worst-case scenario. In this topic, the main idea focuses on Response Surface Methodology (RSM) with second-order models to predict a mathematical model related to the engagement for the whole operational volume [1,2].

1.1.3 Design of Experiments

Design of Experiments (DoE), especially Response Surface Methodology (RSM) has been applied to many engineering problems. These studies include some statistical processes in order to investigate that inputs have the greatest effect on the outputs; at what condition the results will satisfy the customer requirements, and how it can be optimized [5,6]. These methods may be used for both physical testing, as well as simulation testing. However, in aerospace applications of DoE is generally simulation based since the cost associated with actual tests is prohibitive. In aerospace studies, these methods are generally used for design optimization of a single discipline such as aerodynamics [7-11], structures and materials [11-14], propulsion and engine [15,16], trajectory [10] or optimizing many of these disciplines together (i.e., multidisciplinary optimization [17-21]), modeling of complex systems, and reliability analysis.

DoE comprise several kinds of methods but, aside from RSM, they can be divided in two main categories: Factorial designs and Taguchi methods. Factorial designs may further be classified as a full factorial one, where all possible combinations of the factors and levels are investigated, or a fractional factorial design [1].

Table 1 Different Type of Fractional Factorial Designs

Type of Factorial Design	Graph	Formulae			
Full Factorial		A	B	C	Name
		-	-	-	I
		+	-	-	A
		-	+	-	B
		-	-	+	C
		+	+	-	AB
		+	-	+	AC
		-	+	+	BC
+	+	+	ABC		
First Fractional Factorial		A	B	C	Name
		-	-	-	I
		-	-	+	C
		+	+	-	AB
+	+	+	ABC		
Second Fractional Factorial		A	B	C	Name
		-	+	-	B
		-	+	+	BC
		+	-	-	A
+	-	+	AC		
Third Fractional Factorial		A	B	C	Name
		-	-	+	C
		-	+	-	B
		+	-	-	A
+	+	+	ABC		

The full factorial design is very useful to observe the effects of the factors, since it provides a chance to see their main effects, as well as the interactions between each other. However too many simulations are required. The necessary number of simulations to cover all the combinations may be found from n^k , where ‘n’ is the number of factor levels and ‘k’ is the number of factors. Generally factor levels are shown as “-1” for minimum, “0” for average and “+1” for maximum. [2].

In fractional factorial designs, all possible combinations of the factors and levels are not investigated. Naturally, this situation causes a decrease in the accuracy of the analysis, but it is an effective method if the number of factors is too high. In this case, the required simulation runs can be formulated as n^{k-m} , where ‘m’ is the number of fractions [1]. Depending on the number of fractions, the required number of simulations in this case may also be too many. Some fractional factor examples for three factors are given in Table 1 [22].

Taguchi method uses orthogonal arrays that are a special standard set of arrays used to gain detailed information about effects of factors with the minimum number of experiments [23]. The Taguchi method tests pairs of combinations, instead of testing all possible combinations like the factorial designs. The required factor combinations for experiments can be determined by using an array selector algorithm [1]. An example of this table is shown in Table 2 [24]:

Table 2 Taguchi Design Table

		Number of Parameters (P)																														
		2	3	4	5	6	7	8	9	10	11	12	13	14	15	16	17	18	19	20	21	22	23	24	25	26	27	28	29	30	31	
Number of Levels	2	L4	L4	L8	L8	L8	L8	L12	L12	L12	L12	L16	L16	L16	L16	L32	L32	L32	L32	L32	L32	L32	L32	L32	L32	L32	L32	L32	L32	L32	L32	
	3	L9	L9	L9	L18	L18	L18	L18	L27	L27	L27	L27	L27	L36	L36	L36	L36	L36	L36	L36	L36	L36	L36	L36	L36	L36	L36	L36	L36	L36	L36	
	4	L'16	L'16	L'16	L'16	L'32	L'32	L'32	L'32	L'32	L'32	L'32	L'32	L'32	L'32	L'32	L'32	L'32	L'32	L'32	L'32	L'32	L'32	L'32	L'32	L'32	L'32	L'32	L'32	L'32	L'32	L'32
	5	L25	L25	L25	L25	L25	L50	L50	L50	L50	L50	L50	L50	L50	L50	L50	L50	L50	L50	L50	L50	L50	L50	L50	L50	L50	L50	L50	L50	L50	L50	L50
	6	L64	L64	L64	L64	L64	L64	L64	L64	L64	L64	L64	L64	L64	L64	L64	L64	L64	L64	L64	L64	L64	L64	L64	L64	L64	L64	L64	L64	L64	L64	L64

As a result, Taguchi method, with fewer simulations, provides an important advantage to factorial designs. The Taguchi method is strongly suggested for initial iterations of the studies when the number of factors is between 3 and 50. For effective utilization of the method, there should be hardly any interactions between the factors, and only a few factors should contribute significantly to the response [1].

In this thesis, response-surface based DoE methods are used to investigate the performance of an ADMS. Since this process requires too many simulations through conventional methods, such as structured grid methods, there is a need to find faster approaches to carry out the performance analysis. Also it is required to be accurate with the faster approaches, RSM is seemed better related to other experimental methods, since it can give second order mathematical function in order to model the response. So that, this method is generally used for complex analyses around few factors. Thus, construction and utilization of RSM for performance evaluation is addressed.

Elements and components of an experimental design process can be shown in Figure 3 [25]:

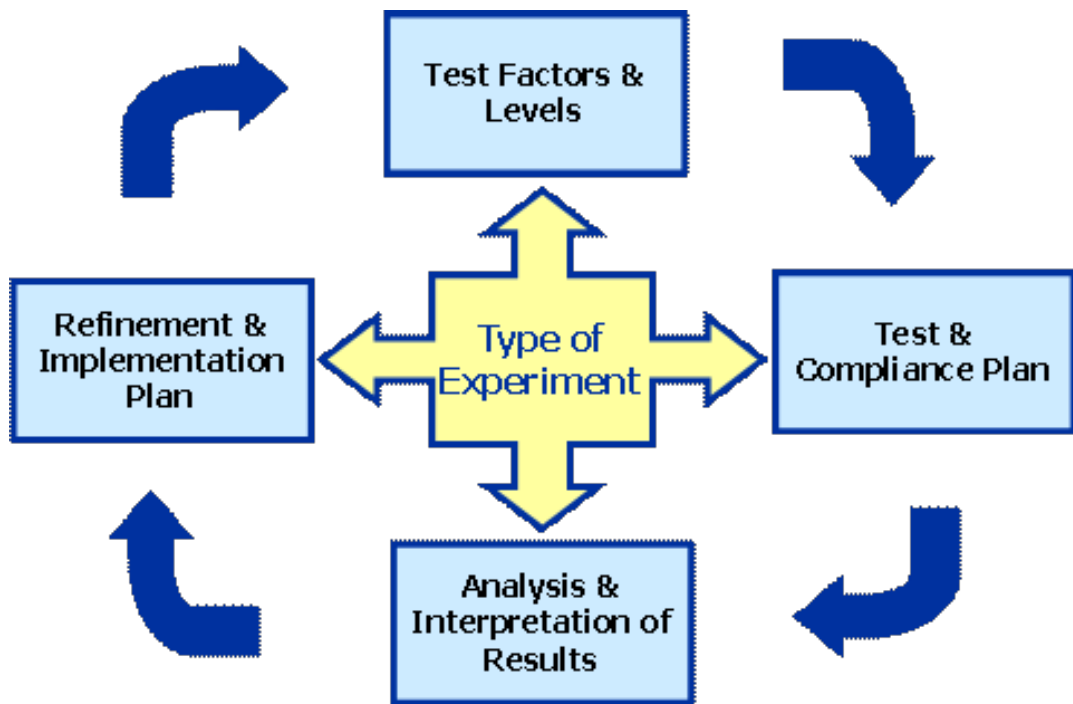


Figure 3 Elements and Components of an Experimental Design Process

As it is mentioned, DoE is a series of methods useful for observing the effects of some controllable and uncontrollable factors on the response. DoE basically investigates answers to questions such as: [3]

- Which experimental analysis method is appropriate?
- How many number of simulation runs are required for the analysis, and can it be minimized?
- What are the optimum conditions?
- How can future analysis be predicted?

While answering these questions, model adequacy should be considered. General adequacy checking methods includes normality tests for checking that data is normally distributed or not and also randomly distributed residuals. An example graph for residual plots regarding to the adequacy check is given in Figure 4 [26]:

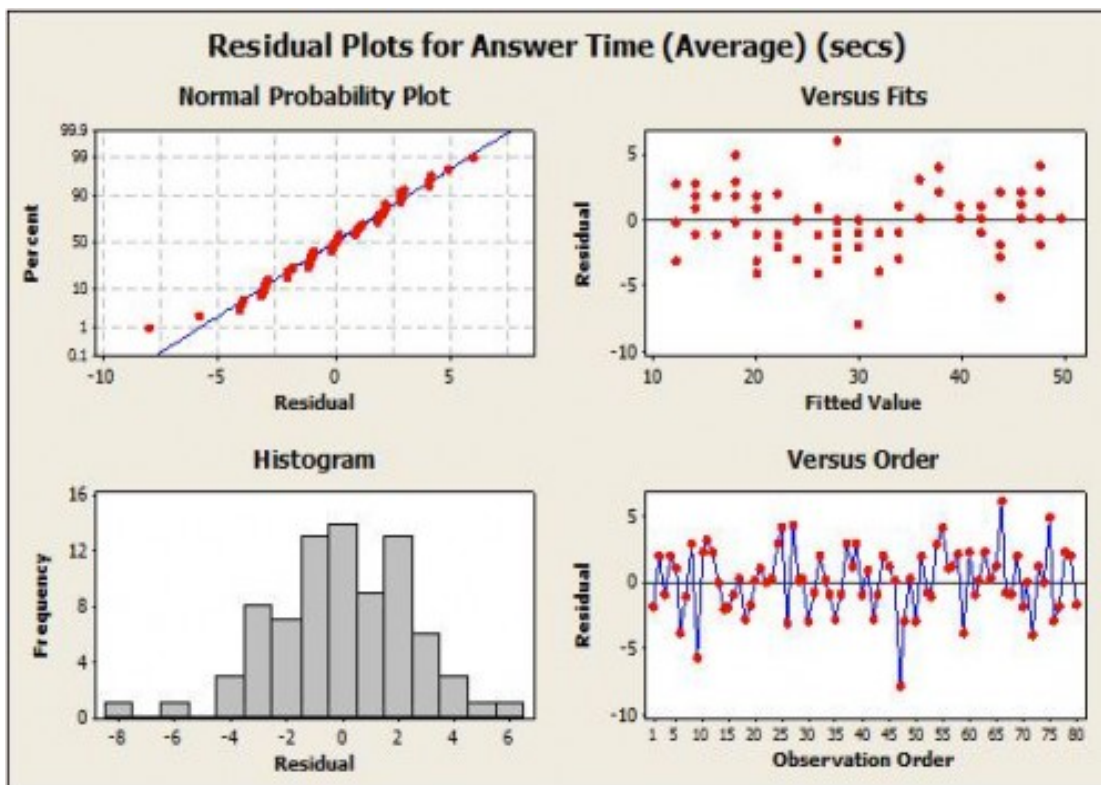


Figure 4 Residual Plots Regarding to the Adequacy Check

There are some statistical tools such as Minitab, JMP and Design Expert etc. for design of experiments including adequacy test tools. In this thesis, Minitab program was chosen for the statistical tool. In Figure 4, there is an example graph for adequacy analysis. There are two expected results from the adequacy tests. One of them is the normality of data, which can be seen on the upper left side of the graph. From graph, experimenter can decide whether data is normally distributed or not by

observation. In another way, experimenter can also decide by using an Anderson-Darling test that determines p-value for normality of data in order to compare with predefined p-value. This will be explained in the next sections. The other adequacy test searches for the residuals are distributed whether randomly or not. This can be seen on the upper right side of the graph. In these graphs, experimenter generally wants to see that data is normally distributed and also the residuals are randomly distributed which means that there is not any specific trend for residuals. [1,2]

1.1.4 Response Surface Method

Response surface modeling involves many steps, such as DoE, conducting or numerical simulation of experiments, construction of the response surface model, and finally adequacy check. DoE may be defined as a test or series of tests in which purposeful changes are applied to the input variables to observe and identify the reasons that cause important changes in the response. At the numerical simulation step, simulations are conducted at conditions determined in the previous step. The construction of the surface model is carried out based on these results. The model helps the experimenter predict possible future results that may be obtained by changing the simulation conditions between ranges of initial analysis bounds. Finally, the adequacy checking is carried out to evaluate whether the constructed model is adequate or whether additional studies are needed. [2] Graphical process of response surface method is given in Figure 5 [27]:

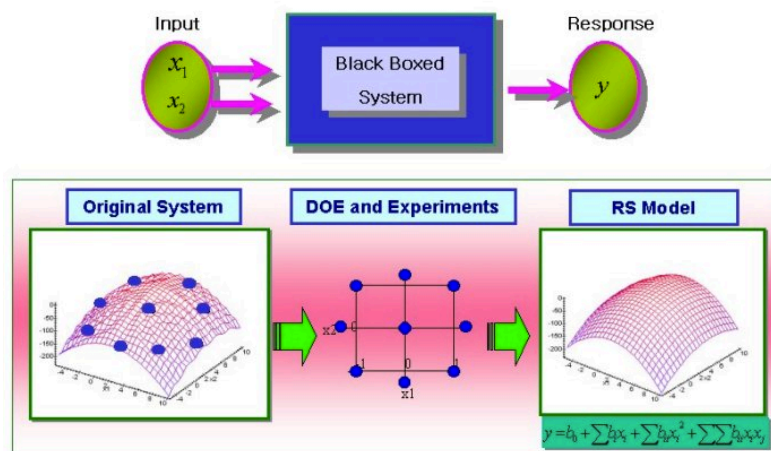


Figure 5 Response Surface Method Process [28]

1.2 Contribution of the Thesis

In this thesis, the response surface methodology is applied to the probability of hit performance prediction of a missile system. To the author's knowledge this application of the RSM is carried out. The effectiveness of the approach is demonstrated through simulations.

1.3 Scope of the Thesis

In Chapter 2, the high fidelity 6-DoF ADMS tool is presented. Since the model is constructed using Matlab / Simulink programming tool, the required analyses are also run in Matlab. Some information about the target scenarios are also given in this section.

In Chapter 3, conventional grid method is explained. Performance analysis is run using a structured grid method. Obtained results are considered as a control scheme for response surface analysis, and they are used to compare PoH outputs.

In Chapter 4, response surface methodology is described. Since the experimental design is created by using Minitab statistical software tool, the required analysis combinations are obtained by using the response surface package of the software. After determining the analysis combinations, experiments are implemented using the ADMS tool carried out. Second order mathematical models are employed to response surfaces. Some goodness of fit tests are also constructed.

In Chapter 5, results obtained from conventional grid method and response surface method for each engagement scenario is compared with each other. The accuracy of the models is observed with the help of these comparisons.

In Chapter 6, the final comments on thesis are made. Also, the alternatives for future work are discussed.

CHAPTER 2

ADMS TOOL AND ENGAGEMENT SCENARIOS

In this chapter, about the Air-Defense Missile System Model (ADMS) is described. In addition, desired engagement scenarios are also given.

2.1 ADMS Tool

Performance assessment of an ADMS is carried out through a high-fidelity six degrees of freedom modeling and simulation tool developed and coded in the MATLAB/Simulink environment. The model contains seven high-level system models. These can be shown as:

- Missile flight simulator that contains the six degrees of freedom missile flight mechanics model and missile avionics containing detailed actuator and sensor models (such as seeker, fuse, gyroscope and accelerometer),
- Launcher system for observing the launcher effects and interaction between missile and launcher
- Radar model for observing ground radar influence,
- Command and control system for threat evaluation and weapon assignment,
- Environment model for testing missile performance in different environmental and terrain conditions.
- Target model for examining missile response against different types of targets and their associated maneuver strategies, and finally
- Engagement model for observing the engagement process

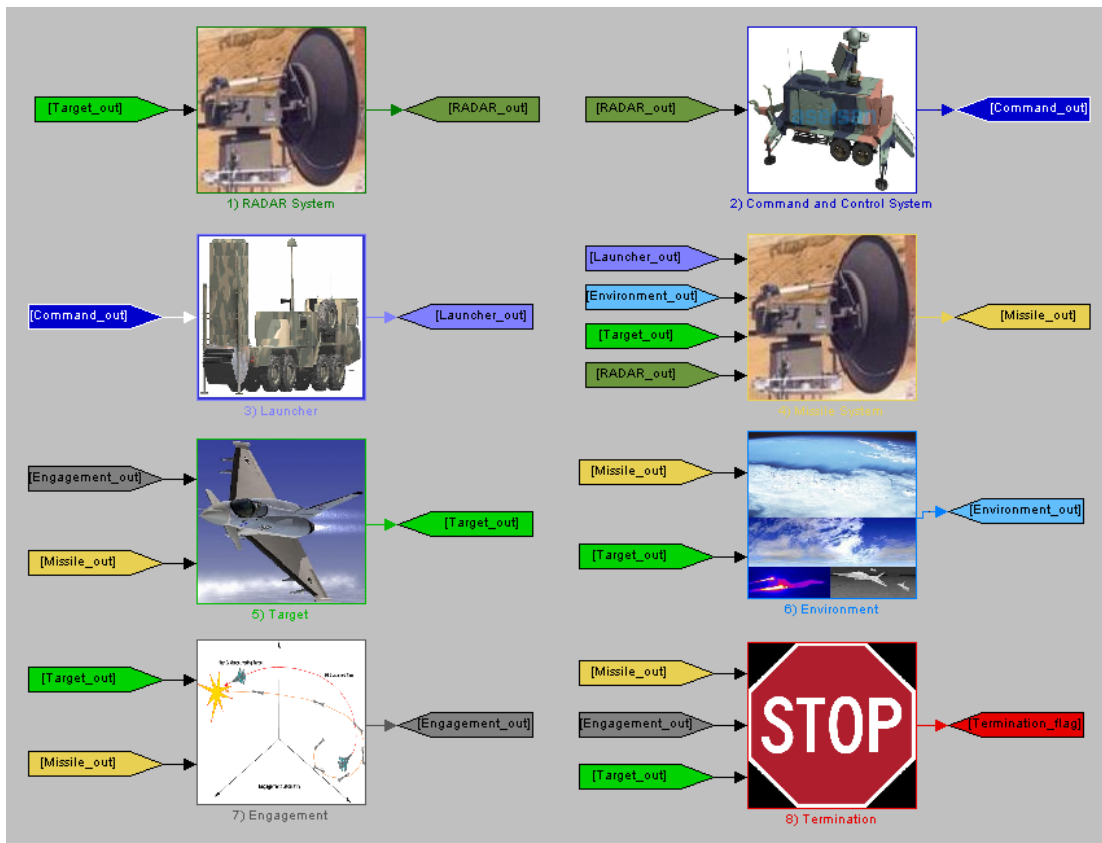


Figure 6 ADMS Tool

These models also include other subsystem models, each of which was put through an extensive validation and verification process. This high-fidelity ADMS modeling and simulation tool has over 1000 parameters for simulating missile-target engagements. Such a high number of model parameters (most of which are either uncertainty or noise parameters within a pre-specified bound such as aerodynamic, control actuation system, propulsion misalignments and offsets; radar, seeker uncertainties and errors) require a very large number of Monte-Carlo simulations in order to estimate expected value of the desired performance.

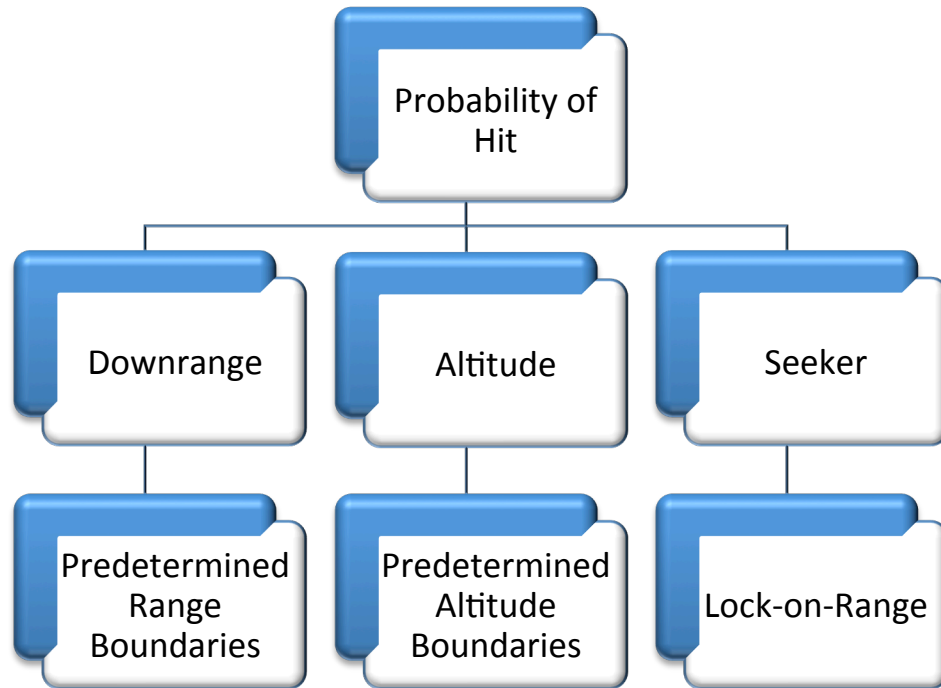


Figure 7 Performance Analysis Tree regarding to Predefined Inputs

The performance parameter considered in this study is the probability of hit (PoH) as given in Figure 7. If the miss distance of the missile during simulation is below a particular value, it is considered a hit. Then, its probability is calculated using

$$\% PoH = \frac{\text{number of hits}}{\text{total runs}} \times 100$$

While running Monte-Carlo runs, the main consideration is focused on three parameters. These are:

- Downrange → Predetermined Range Boundaries
- Altitude → Predetermined Altitude Boundaries
- Seeker → Lock-on-Range Distance

Inclusion of more detail in any of the subsystem models often causes an increase in the number of model parameters, which results in a further increase in the required number of simulation runs. Therefore, the scope of this study is to design an experiment based on response surface methodology for determining the most

effective factors in order to decrease the number of parameters and create response surface models with smallest number of simulations.

The other parameters, errors, and noise values are taken as a Gaussian (normal) distribution with a mean value of 0. For every selected downrange, altitude and LOR combination, a Monte-Carlo simulation is carried out with each containing 500 runs. This Monte-Carlo run number is determined by the experimenter based on the past experience.

2.2 Engagement Scenarios

The purpose of this study is to reduce the required number of computer simulation runs to estimate the PoH values of an ADMS within its operational volume. All the required simulations are conducted using the high-fidelity simulation tool described above. In the Monte-Carlo runs, the effects of three fundamental parameters are considered. These parameters are engagement altitude, engagement downrange, and the missile seeker's lock-on-range (LOR) value. These parameters are selected based on experience, as well as the historical data available on the effect of parameters on missile performance. Performance is analyzed for three different target maneuvering startup ranges and under the consideration of different downrange, altitude and lock-on-range values. For non-maneuvering targets, the simulations are run for the conditions of:

- Engagement downrange is selected to cover between 20-100% of reference range,
- Engagement altitude to cover between 10-50% of reference range, and
- The LOR values are chosen to be between 20-40% of reference range.

And for the maneuvering target analysis conditions:

- Engagement downrange is selected to cover between 24-100% of reference range,
- Engagement altitude to cover between 6-30% of reference range, and
- The LOR values are chosen to be between 12-24% of reference range.

These scenarios are tabulated in Table 3:

Table 3 Table of Scenarios used in the Study

	Non-Maneuvering		Maneuver Startup Range of 12 %		Maneuver Startup Range of 18 %	
	Minimum	Maximum	Minimum	Maximum	Minimum	Maximum
Downrange percent of Reference Range	20%	100%	32.5%	92%	32.5%	92%
Altitude percent of Reference Range	10%	50%	12%	24%	12%	24%
Lock-on- Range (LOR)	20%	40%	12%	24%	12%	24%

The experimental designs are prepared with respect to different engagement scenarios. For each scenario, the target is assumed to have constant velocity and same maneuver type. In addition, target is assumed to know that it has been engaged by the missile, with perfect knowledge of the missile's current position. For the maneuvering cases, they are employed to simulate the best escape scenarios. Thus, the evasive maneuvers are always carried out with respect to the missile position in order to enforce the missile to pursue with high-g maneuvers, as discussed in the previous section. At every run, the associated Monte-Carlo variables (such as thrust misalignments, radar errors, aerodynamic coefficient uncertainties, etc.) are signed randomly with an algorithm. The threshold missile-target proximity value to assume a hit is selected to be 5 meters.

If the miss distance of the missile during simulation is below 5 meters, it is considered a hit. Then, its probability is calculated using

$$PoH\% = \frac{\#hits}{\#runs} \times 100$$

where;

#hits is the number of simulations runs assumed as hit, and

#runs is the number of total simulation runs

In this study, two approaches are considered. The first approach is the conventional grid analysis approach, where Monte-Carlo runs at uniformly distributed grid points are carried out. The other approach is the response surface approach, where second-order models are considered in this project.

CHAPTER 3

GRID METHODOLOGY FOR PERFORMANCE ANALYSIS

This chapter of the thesis is devoted to clarifying the grid methodology steps for analyzing missile performance via MATLAB. Definitions regarding to the grid approach for the engagement scenarios are given.

3.1 Non-Maneuvering Scenarios

In the conventional grid analysis method, a set of uniformly distributed grid points, as shown in Figure 8, are selected in the operational area. Then Monte-Carlo runs, with 500 simulations in each run, are carried out using the missile simulation model. The number of Monte-Carlo runs is:

$$\begin{aligned} & 9 \text{ (downranges) } \times 5 \text{ (altitude) } \times 3 \text{ (LOR)} \\ & = 135 \text{ Monte - Carlo runs} \end{aligned}$$

Then the number of simulations run required becomes:

$$135 \times 500 = 67,500$$

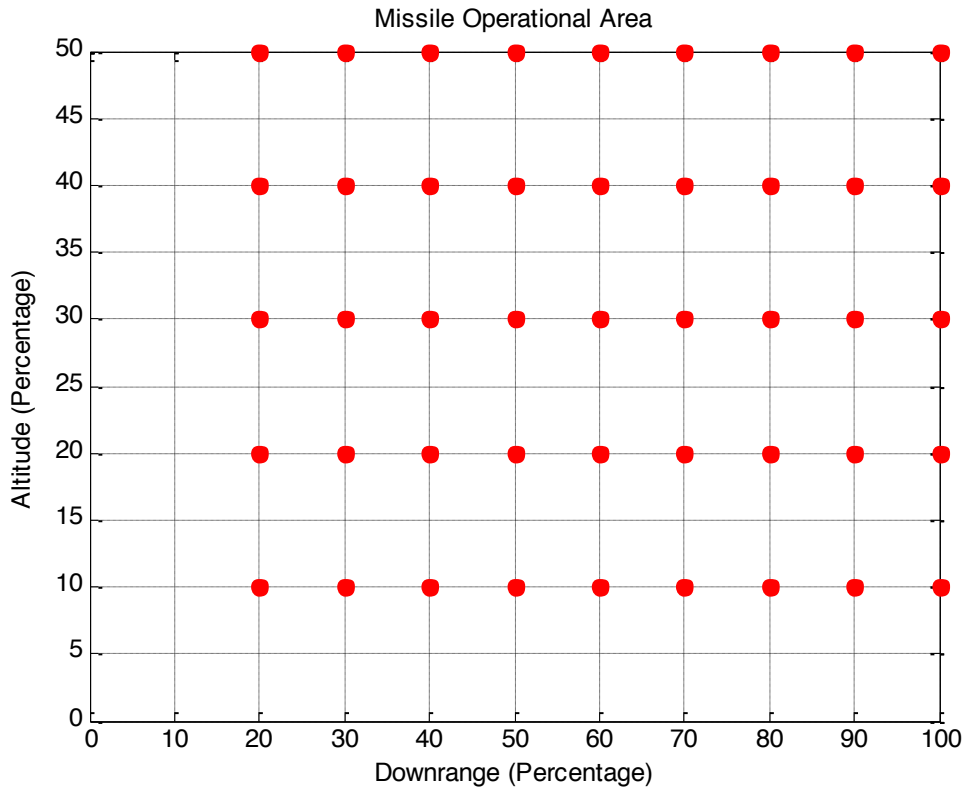


Figure 8 Missile Operational Areas for the Non-Maneuvering Target Case

Missile operational area is given in Figure 8. As it is seen, the sampling points are selected as a structured grid. And the range between the points in both downrange and altitude axis is set to %10. In addition, the sampling points are aligned with %10 starting from %20 to %40.

All the Monte-Carlo runs are done for each sampling points by using ADMS modeling and simulation tool developed. After obtaining the probability of hit results, the graphs for each combination of downrange, altitude and Lock-on-Range are plotted.

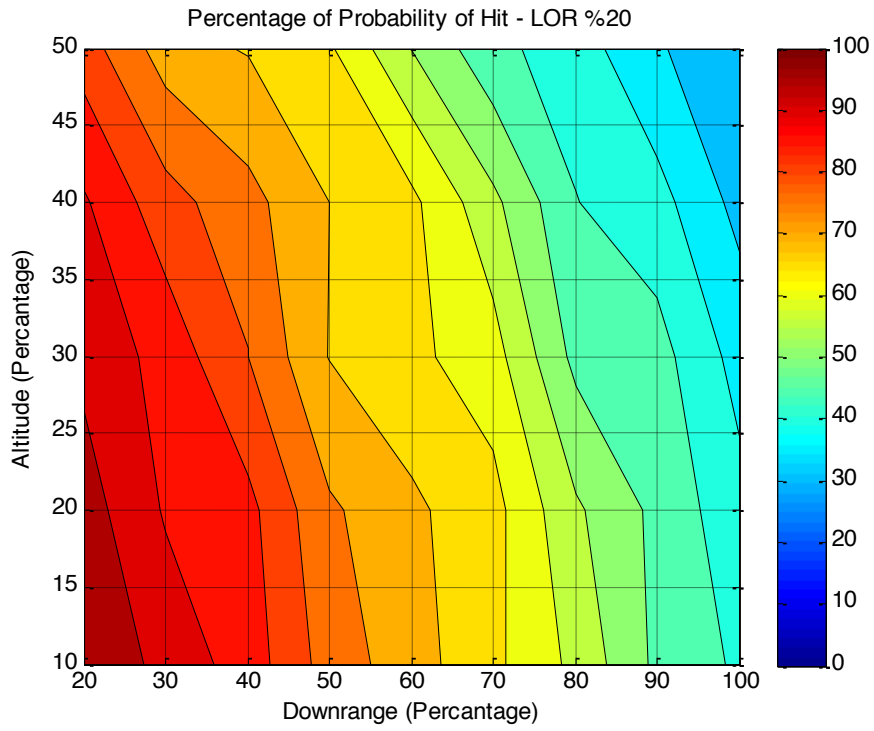


Figure 9 PoH Results for GRID approach for Non-Maneuvering Case at LOR %20

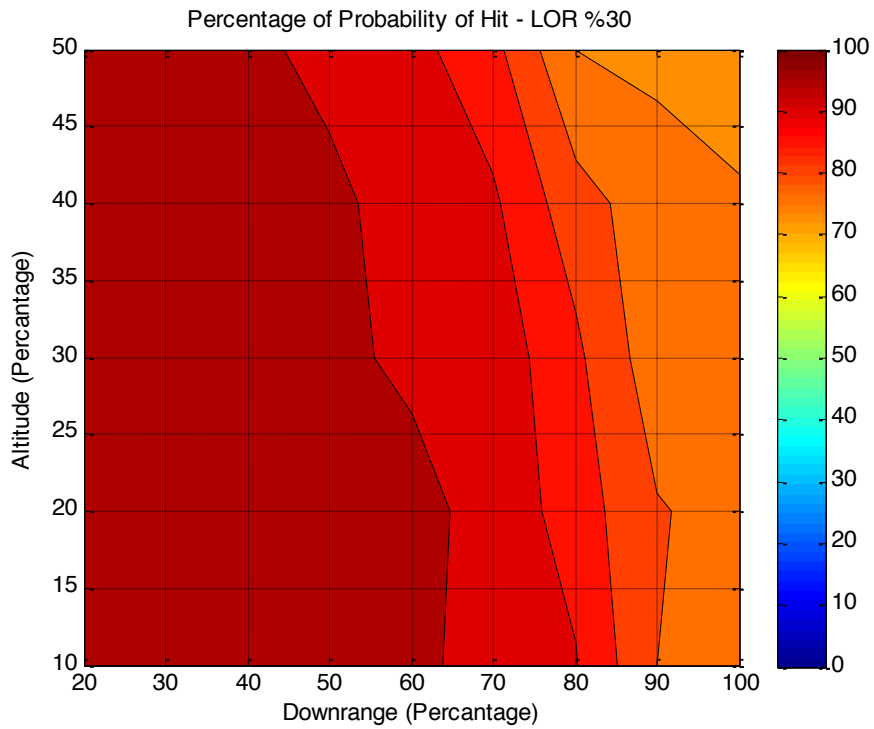


Figure 10 PoH Results for GRID approach for Non-Maneuvering Case at LOR %30

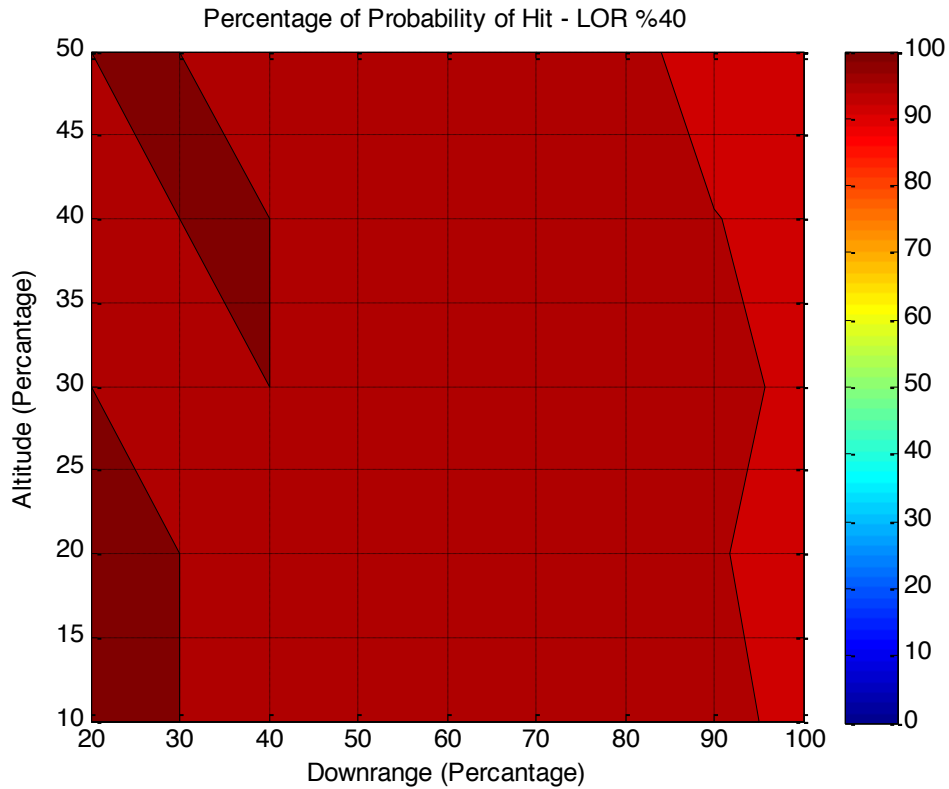


Figure 11 PoH Results for GRID approach for Non-Maneuvering Case at LOR %40

As it is seen from the probability of hit figures, while the percentage of lock-on-range is increasing, the percentage of probability of hit also increases. Especially for the value of %40 LOR and above, the system reaches nearly to %100. In addition, PoH value decreases when the downrange is increased. It means that the missile system has a better effect for the closer target scenarios. Furthermore, if the altitude is increased, then the PoH value goes down. So that it has also negative effect on missile performance but not as much as the other parameters. It can be said that the most effective parameter on missile performance is lock-on-range value. Downrange value follows the lock-on-range value, and altitude seems to be the least significant parameter for the missile performance in the case of non-maneuvering target.

3.2 Maneuvering Scenarios

As in the grid analysis method for non-maneuvering targets, a set of uniformly distributed grid points, as shown in Figure 12, are selected in the operational area. Then Monte-Carlo runs, with 500 simulations in each run, are carried out using the missile simulation model. The number of Monte-Carlo runs is:

$$10(\text{downranges}) \times 5 (\text{altitude}) \times 3 (\text{LOR}) \\ = 150 \text{ Monte - Carlo runs}$$

$$150(\text{Monte - Carlo}) \times 2 (\text{Maneuver Types}) = 300 \text{ Total Runs}$$

Then the number of simulations run required thus becomes

$$300 \times 500 = 150,000$$

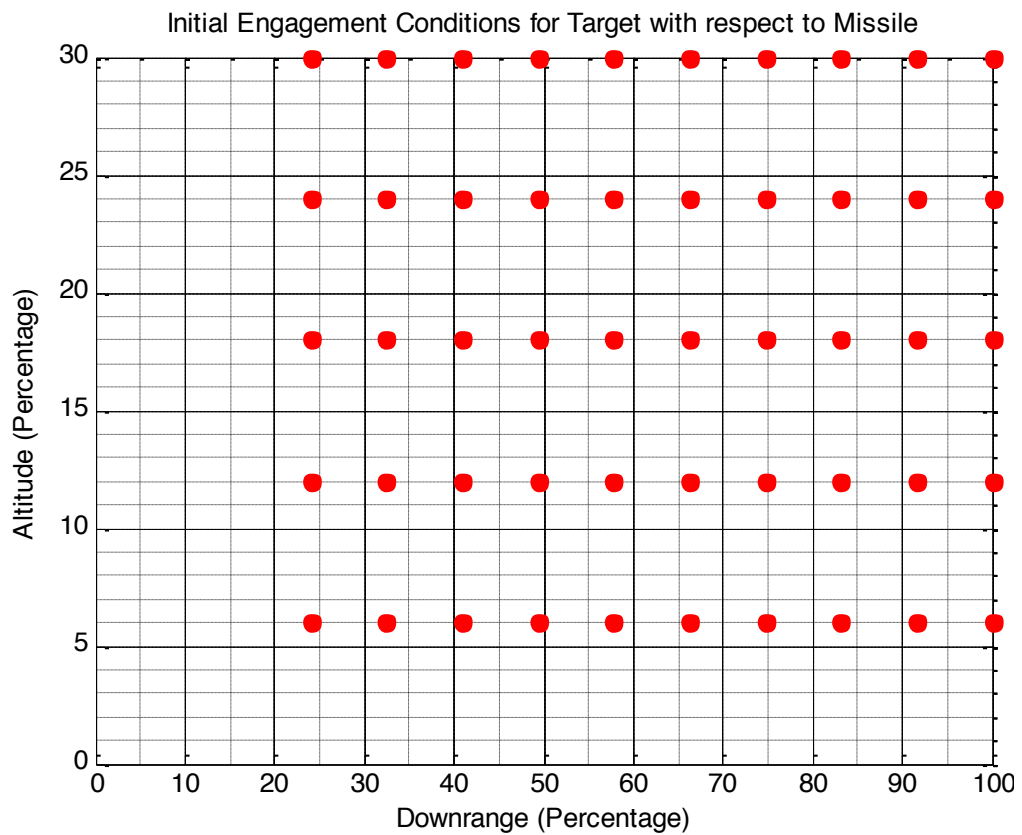


Figure 12 Missile Operational Areas for Maneuvering Cases

Missile operational area is given in Figure 8. As it is seen, the sampling points are selected as a structured grid. But there is a difference between the non-maneuvering and maneuvering targets sampling periods. For the maneuvering cases, sampling period is %8.5 in downrange axis and %6 in altitude axis. Furthermore, sampling period of LOR value is set to %6 starting from %12 to %24.

LOR values between %12 - %24 for the maneuvering conditions can be assumed as same with the LOR values of %20 - % 40 for the non-maneuvering case, since the reference range which is named as the max value of the downrange is expanded.

All the Monte-Carlo runs are done for each sampling points by using ADMS modeling and simulation tool in Matlab / Simulink. After obtaining the probability of hit results, the graphs for each combination of downrange, altitude and Lock-on-Range is drawn.

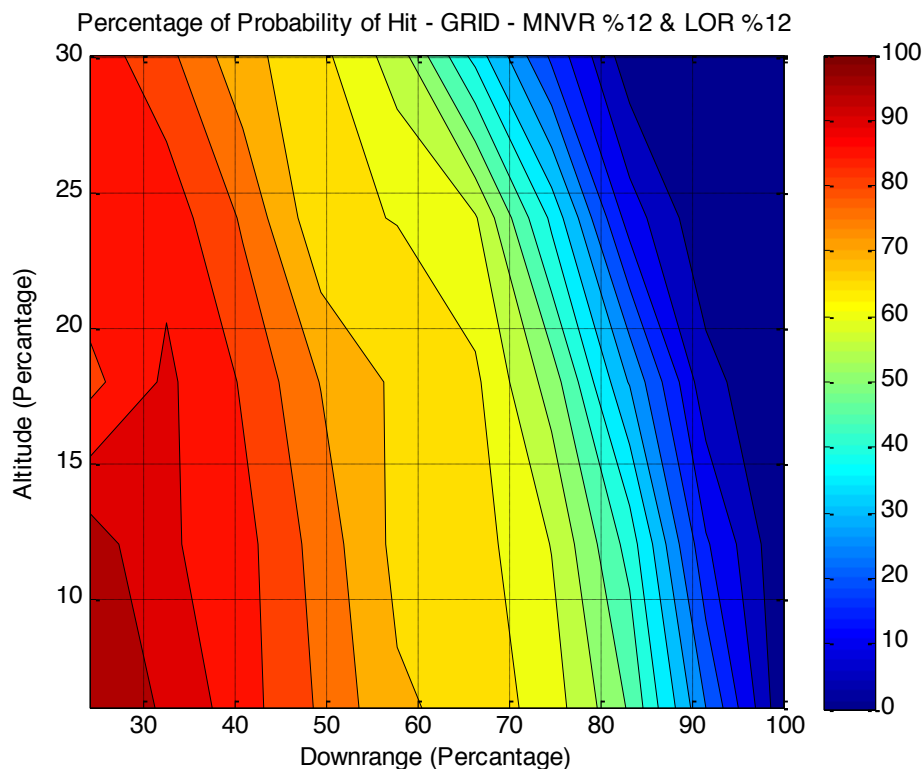


Figure 13 PoH Results for GRID approach for Maneuver Start-up Range %12 at LOR % 12

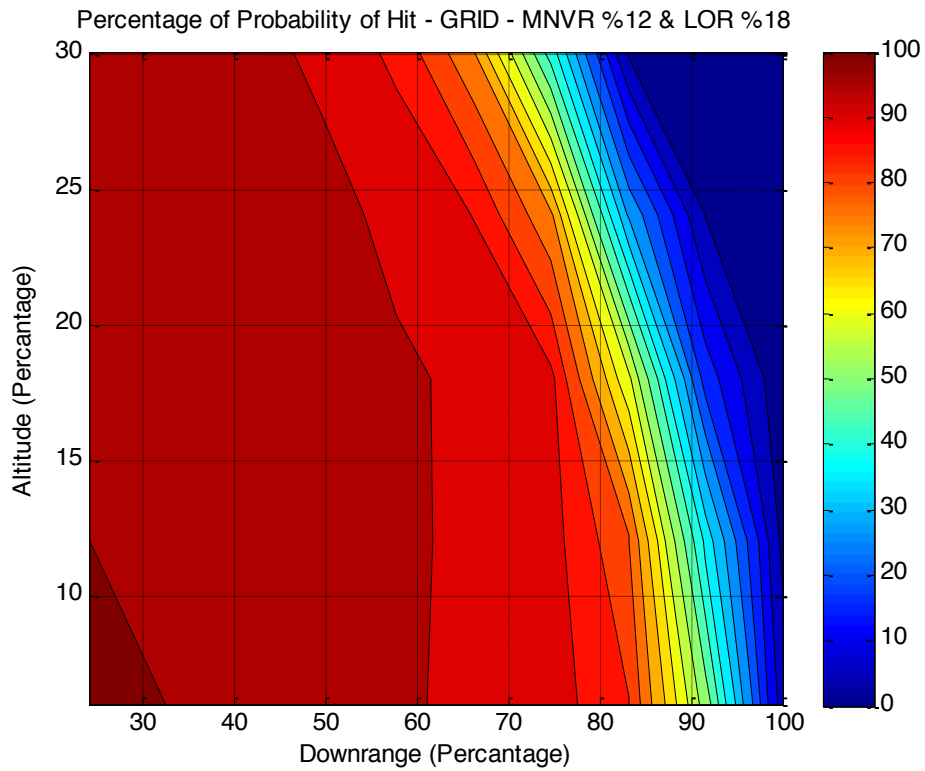


Figure 14 PoH Results for GRID approach for Maneuver Start-up Range %12 at LOR % 18

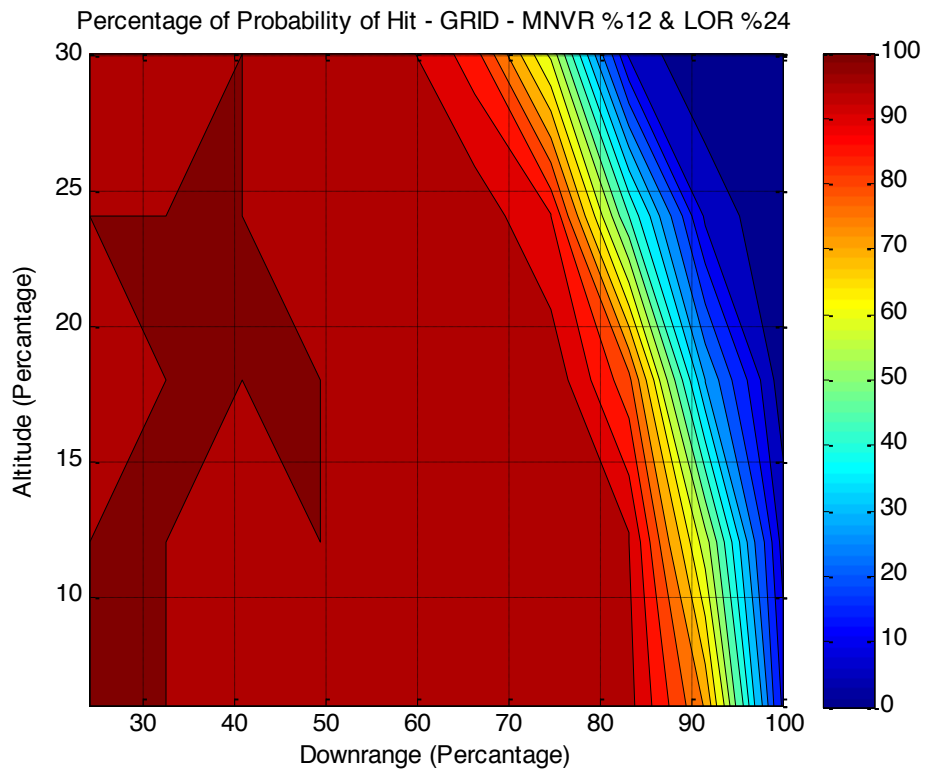


Figure 15 PoH Results for GRID approach for Maneuver Start-up Range %12 at LOR % 24

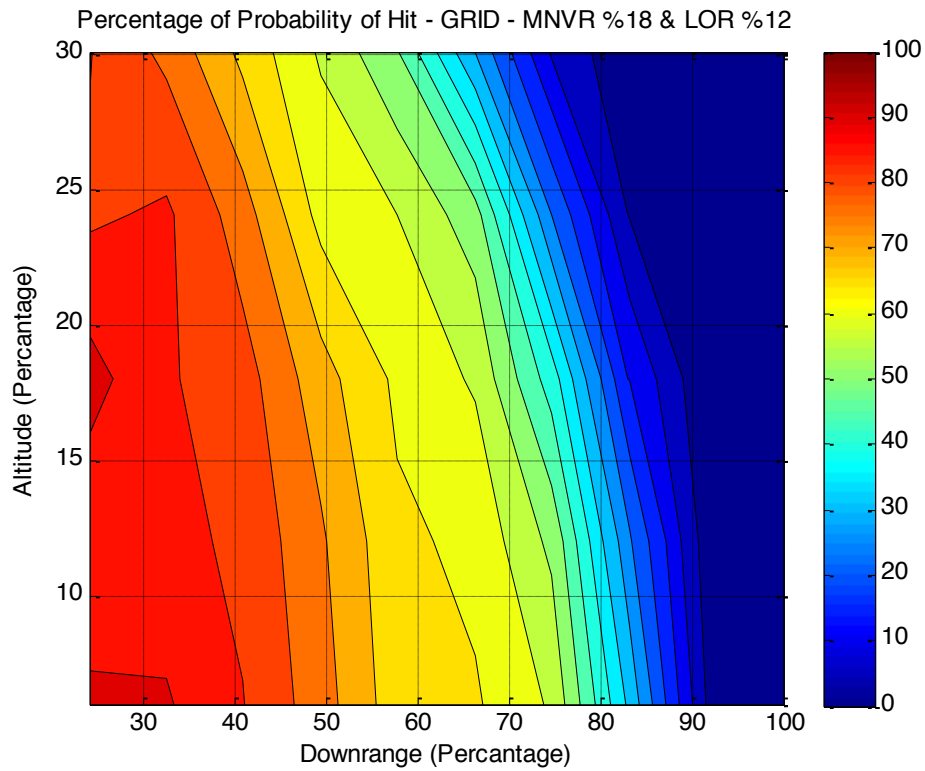


Figure 16 PoH Results for GRID approach for Maneuver Start-up Range %18 at LOR % 12

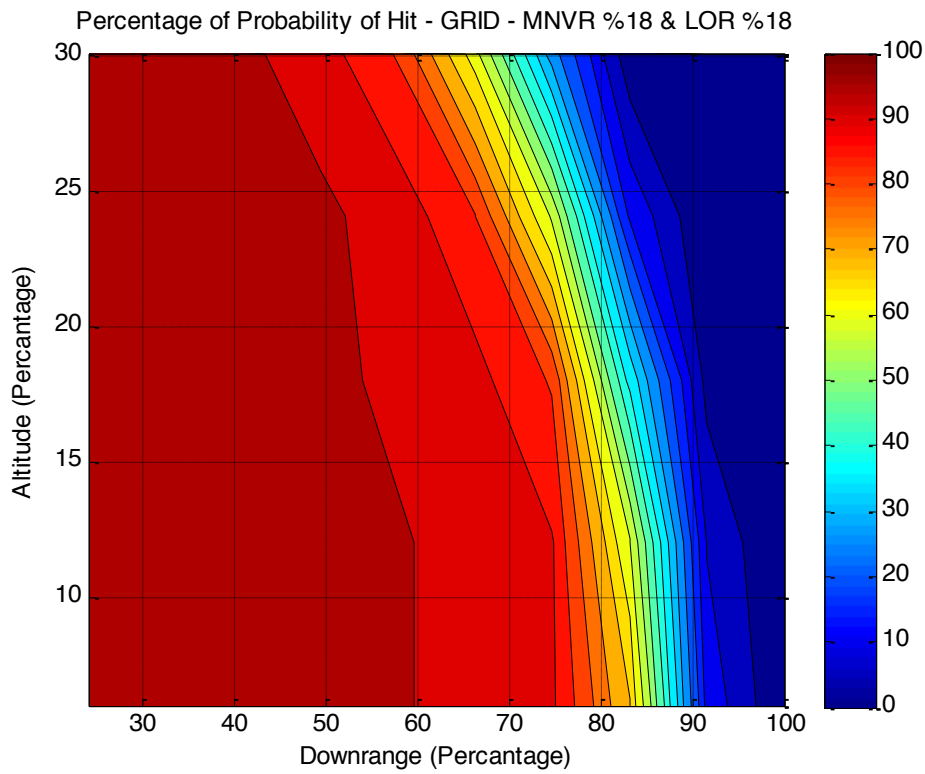


Figure 17 PoH Results for GRID approach for Maneuver Start-up Range %18 at LOR % 18

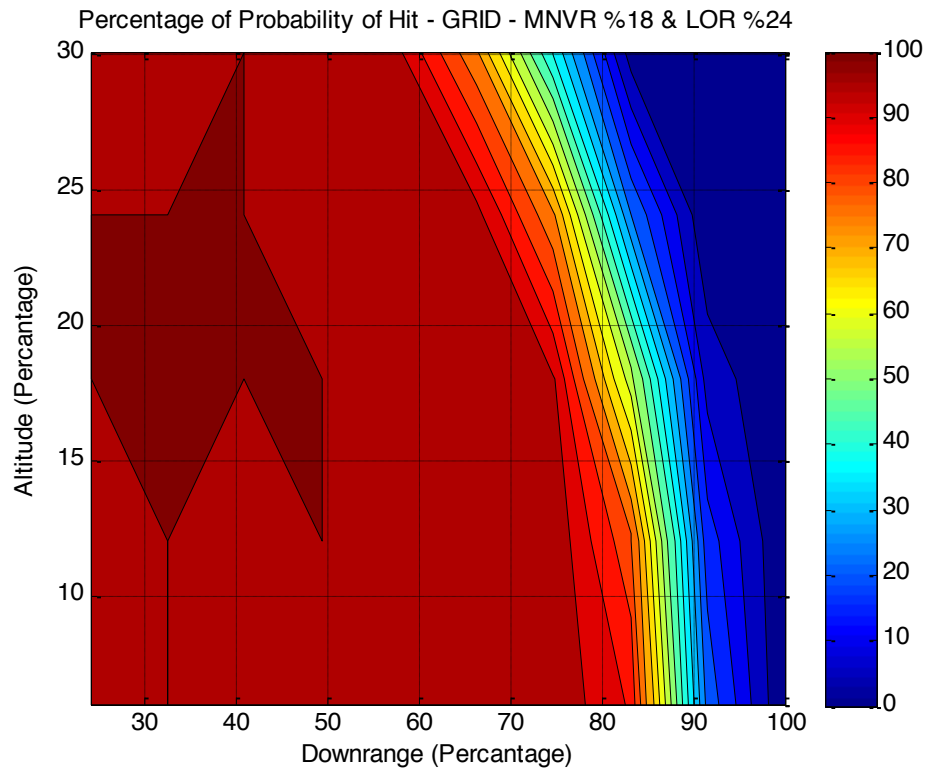


Figure 18 PoH Results for GRID approach for Maneuver Start-up Range %18 at LOR % 24

As it is seen from the probability of hit figures, while the percentage of lock-on-range is increasing, the percentage of probability of hit also increases. But there is not a similar result with the non-maneuvering case at %40 LOR and maneuvering cases for %24 LOR, since maneuvering complicates to chase. In addition, PoH value decreases when the downrange is increased. It means that the missile system has a better effect for the closer target scenarios. Furthermore, if the altitude is increased, then the PoH value goes down. So that it has also negative effect on missile performance but not as much as the other parameters. It can be said that the most effective parameter on missile performance is still lock-on-range value. Downrange value follows the lock-on-range value, and altitude seems to be the least significant parameter for the missile performance also in the cases of maneuvering target.

CHAPTER 4

RESPONSE SURFACE METHODOLOGY BASED DESIGN OF EXPERIMENTS

In this chapter, after giving some information about the formulation of the response surface designs, fundamentals about the response surface methodology based design of experiments are defined and the motivation behind the idea of the response surface approach is defined.

4.1 Formulation of Response Surface Methodology

Response surface methodology is totally based on the idea of regression analysis. Supposing that a response of a function denoted as “y” changes under the influence of “n” factors also called as “independents” or “regressor variables”. The relationship between these variables is characterized by a mathematical model called as “regression model” [1,2].

The frequently used area of the regression models are for “unplanned experiments” that can be stated as some historical records about the problems or unplanned observations [1,2].

Mathematical model of regression analysis can be shown as:

$$\begin{aligned} y_i &= \beta_0 + \beta_1 x_{i1} + \beta_2 x_{i2} + \dots + \beta_k x_{ik} + \epsilon_i \\ &= \beta_0 + \sum_{j=1}^k \beta_j x_{ij} + \epsilon_i \quad i = 1, 2, \dots, n \end{aligned}$$

By using least squares method:

$$L = \sum_{i=1}^n \epsilon_i^2 = \sum_{i=1}^n \left(y_i - \beta_0 - \sum_{j=1}^k \beta_j x_{ij} \right)^2$$

$$\frac{\partial L}{\partial \beta_0} \Big|_{\hat{\beta}_0, \hat{\beta}_1, \dots, \hat{\beta}_k} = -2 \sum_{i=1}^n \left(y_i - \hat{\beta}_0 - \sum_{j=1}^k \hat{\beta}_j x_{ij} \right) = 0$$

Simplifying the obtained formulas called as “least squares normal equations”:

$$y = X\beta + \epsilon$$

Where;

$$y = \begin{bmatrix} y_1 \\ y_2 \\ \vdots \\ y_n \end{bmatrix}, X = \begin{bmatrix} 1 & x_{11} & x_{12} & \dots & x_{1k} \\ 1 & x_{21} & x_{22} & \dots & x_{2k} \\ \vdots & \vdots & \vdots & \ddots & \vdots \\ 1 & x_{n1} & x_{n2} & \dots & x_{nk} \end{bmatrix}, \beta = \begin{bmatrix} \beta_1 \\ \beta_2 \\ \vdots \\ \beta_n \end{bmatrix}, \epsilon = \begin{bmatrix} \epsilon_1 \\ \epsilon_2 \\ \vdots \\ \epsilon_n \end{bmatrix}$$

It is required to find the least squares estimators, $\hat{\beta}$, that minimizes:

$$L = \sum_{i=1}^n \epsilon_i^2 = \epsilon' \epsilon = (y - X\beta)'(y - X\beta)$$

L can be defined as:

$$L = y'y - \beta'X'y - y'X\beta + \beta'X'X\beta$$

$$= y'y - 2\beta'X'y + \beta'X'X\beta$$

Noting that; $\beta'X'y$ is a scalar, so its transpose will also same $\rightarrow (\beta'X'y)' = y'X\beta$

This results that the least squares estimator of β is

$$\frac{\partial L}{\partial \hat{\beta}} \Big|_{\hat{\beta}} = -2X'y + 2X'X\hat{\beta} = 0$$

$$X'X\hat{\beta} = X'y \xrightarrow{\text{yields}} \hat{\beta} = (X'X)^{-1}X'y$$

Thus the fitted regression model will be;

$$\hat{y} = X\hat{\beta}$$

Residuals can be stated as:

$$e = y - \hat{y}$$

For the estimation of variance, σ^2 , sum of squares of the residuals can be used:

$$SS_E = \sum_{i=1}^n (y_i - \hat{y}_i)^2 = \sum_{i=1}^n e_i^2 = e'e$$

Then by replacing with, $e = y - \hat{y} = y - X\hat{\beta}$;

$$\begin{aligned} SS_E &= (y - X\hat{\beta})'(y - X\hat{\beta}) \\ &= y'y - \hat{\beta}'X'y - y'X\hat{\beta} + \hat{\beta}'X'X\hat{\beta} \\ &= y'y - 2\hat{\beta}'X'y + \hat{\beta}'X'X\hat{\beta} \end{aligned}$$

Since $X'X\hat{\beta} = X'y$; sum of squares errors will be;

$$SS_E = y'y - \hat{\beta}'X'y$$

Because, sum of squares errors has $(n-p)$ degrees of freedom, variance σ^2 will be:

$$E(SS_E) = \sigma^2(n - p) \xrightarrow{\text{yields}} \sigma^2 = \frac{SS_E}{n - p}$$

Response surface methodology (RSM) is a collection of statistical and mathematical techniques that are useful for the modeling and analysis of problems in which a response of interest by several variables and the objective is to develop, improve and optimize the processes [1,2].

Response surface designs are generally used for:

- Factor screening
- Response optimization
- Obtaining detailed information about the response under the influence of factors with minimum simulations

Any process response depends on “n” factors can be formulated as:

$$y = f(x_1, x_2, \dots, x_n) + \epsilon$$

Where;

ϵ : The noise or error observed in the response and this term is assumed to distribute normally with zero mean and have a variance σ^2 .

If the expected response is denoted as;

$$E(y) = f(x_1, x_2, \dots, x_n) = \eta$$

Called as a “response surface”. [4,6]

Because, the real response of the system or function is unknown, it must be estimated or converged. In many cases, usually either a “first-order model” or a “second-order model” is used. For the case of independent variables, a first-order model is appropriate:

$$y = \beta_0 + \beta_1 x_1 + \beta_2 x_2 + \dots + \beta_n x_n + \epsilon$$

This first-order model is sometimes called as a “main effects model” since it has only the main effects of the factors. If there is an interaction between the factors it can be easily added to model as: [4,6]

$$y = \beta_0 + \beta_1x_1 + \beta_2x_2 + \dots + \beta_nx_n + \beta_{12}x_1x_2 + \dots + \beta_{1n}x_1x_n + \dots + \beta_{(n-1)n}x_{(n-1)}x_n + \epsilon$$

If there is any curvature in the real response of the function, then first-order model is not enough, so that a second-order model is generally used in these cases: [4,6]

$$y = \beta_0 + \beta_1x_1 + \beta_2x_2 + \dots + \beta_nx_n + \beta_{11}x_1^2 + \beta_{22}x_2^2 + \dots + \beta_{nn}x_n^2 + \beta_{12}x_1x_2 + \dots + \beta_{1n}x_1x_n + \dots + \beta_{(n-1)n}x_{(n-1)}x_n + \epsilon$$

The second-order model is widely used in response surface methodology because of: [4,6]

It usually works well as an approximation to the real response surface because of the flexibility of the second-order model.

The estimation of the parameters (the β 's) in the second-order model is easy; in addition a well-known method called as least squares can be used for this purpose. This situation provides that there is a close connection between RSM and linear regression analysis.

Mostly used response surface designs, Central Composite (CCD) and Box-Behnken, are shown in Figure 19, respectively [3]:

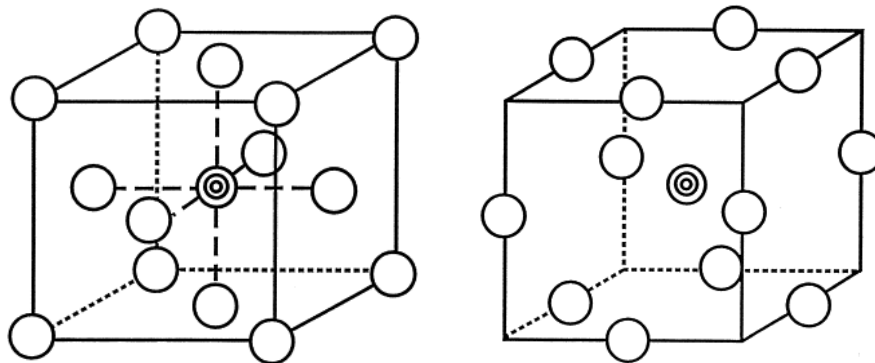


Figure 19 Sample Locations for Response Surface Construction: Central Composite (left) and Box-Behnken (right)

4.2 Response Surface Design Process

Process for the response surface design is similar to the general design of experiments process. First of all, the objectives and the inputs are defined in order to set the responses and factors. After that, appropriate experimental design methods is selected, in this case response surface method is the most preferable one. After, designing the experiment via statistical tools, data collection phase starts. With using the collected data, model is constructed in order to obtain mathematical function for the design space. Adequacy checking is satisfied for the data in order to control the compatibility of the design. Finally, the prediction phase via constructed models is carried out. Simple process loop of an experimental design project is shown in Figure 20:

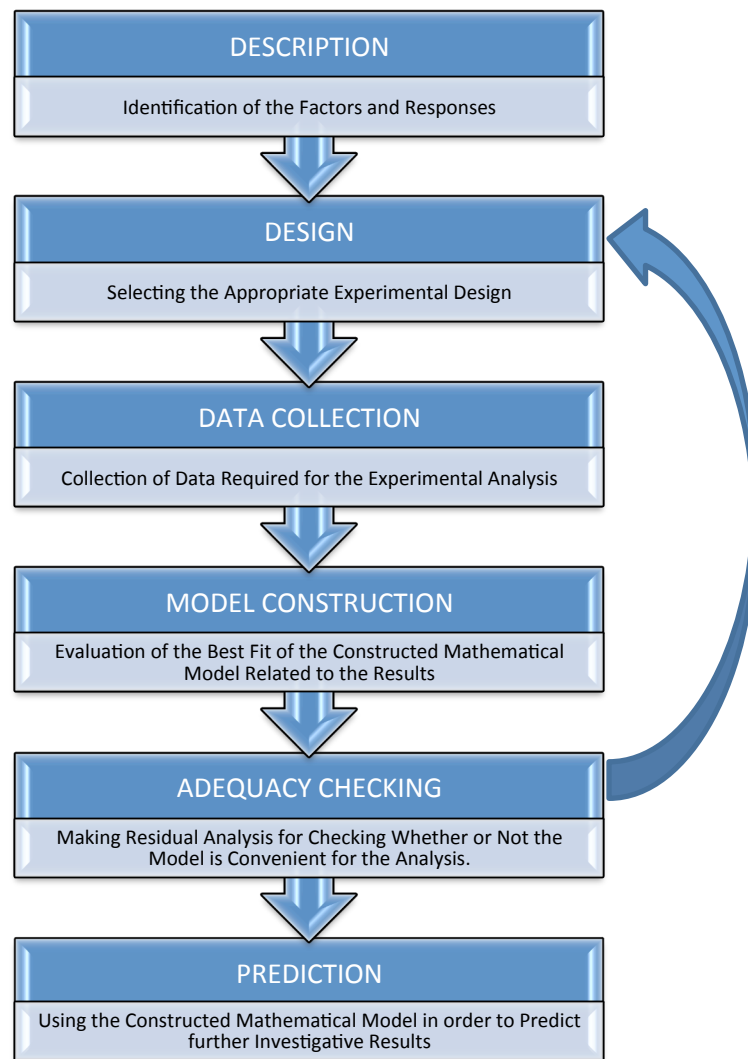


Figure 20 Response Surface Based Experimental Design Project Process Loop

4.3 RSM Approach to Performance Analysis Problem

First alternative method compared to the normal grid analysis is response surface analysis. Here, central composite sampling or experimental design is used. The required sampling points are obtained using the statistical analysis program called Minitab, within the input bounds. This general-purpose software may be used for performing statistical analysis, ANOVA analysis, regression model construction, quality analysis as well as DoE. Data distribution tests may also be carried out by Minitab, such as normality, correlation and covariance. The code can also present the analysis results graphically. These results may also be examined by using p-values. At the beginning of the analysis, the experimenter selects a threshold value, and obtained p-values are compared to the predetermined threshold value. This threshold value shows the risk level that can be acceptable for the analysis. For the condition that the obtained p-value is larger than the threshold value, it can be said that if the experimenters chose the alternative hypothesis, they will take a risk more than they can accept. So, they select the zero hypotheses. In contrast, for the condition that the p-value is smaller than the threshold value, it can be said that if the experimenters select the alternative hypothesis, they will take a risk less than the limit. So, they choose the alternative hypothesis and reject the zero hypotheses.

Since the range is twice the value of altitude, it is divided in two, to obtain two separate response surfaces for low range and high range parts of the operation area. Since the operational area is not so small; if the whole operational area is examined at the same time, the resulting response surface model will not be adequate to represent the performance. On the other hand, separation number can be increased for the larger operational area analysis. Although this process increases the run number, it increases the accuracy of the analysis and the adequacy of the mathematical model. This separation can be done based on previous experiments.

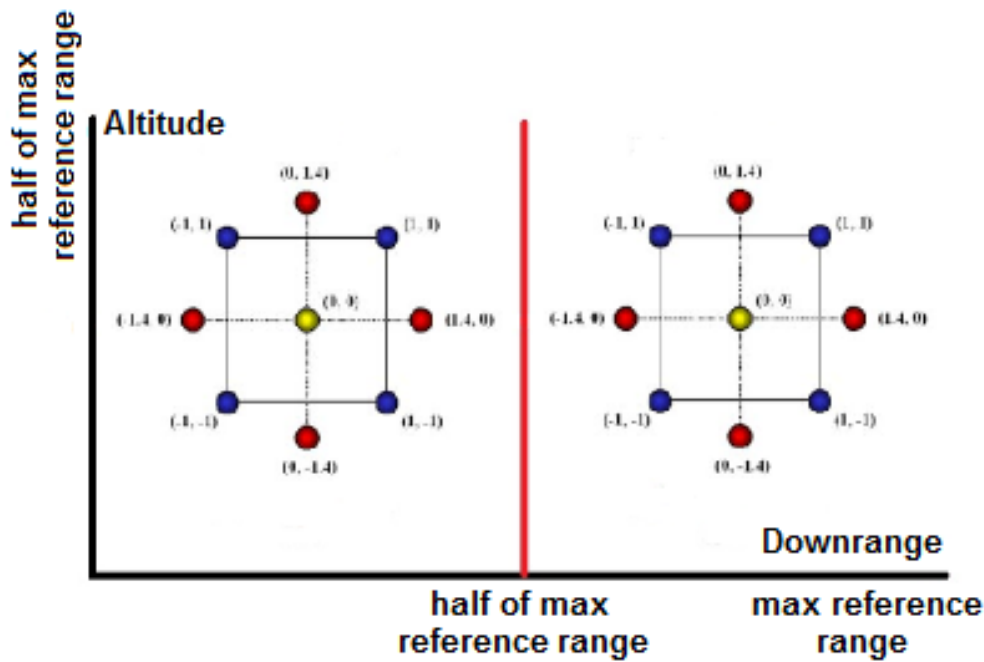


Figure 21 Division of the operation area for RSM Construction

4.3.1 RSM Approach for Non-Maneuvering Case

Two central composite sample point designs are made with same factors but different values. The necessary minimum and maximum values of the selected factors, determined by Minitab, are chosen in such a way that they contain the whole parameter value space as the ones like in normal grid analysis. Necessary parameter combinations for performance analyze via response surface methodology for each design part are given in figures:

Table 4 First Part of the Domain with CCD for Non-Maneuvering Case

↓	C1	C2	C3	C4	C5	C6	C7	C8
	StdOrder	RunOrder	PtType	Blocks	Altitude (%)	Downrange (%)	LOR (%)	PoH (%)
1	1	1	1	1	15.0000	15.0000	20.0000	98.0
2	2	2	1	1	40.0000	15.0000	20.0000	85.6
3	3	3	1	1	15.0000	40.0000	20.0000	75.4
4	4	4	1	1	40.0000	40.0000	20.0000	72.4
5	5	5	1	1	15.0000	15.0000	40.0000	100.0
6	6	6	1	1	40.0000	15.0000	40.0000	100.0
7	7	7	1	1	15.0000	40.0000	40.0000	99.8
8	8	8	1	1	40.0000	40.0000	40.0000	99.8
9	9	9	-1	1	6.4776	27.5000	30.0000	99.6
10	10	10	-1	1	48.5224	27.5000	30.0000	97.2
11	11	11	-1	1	27.5000	6.4776	30.0000	99.8
12	12	12	-1	1	27.5000	48.5224	30.0000	96.2
13	13	13	-1	1	27.5000	27.5000	13.1821	38.4
14	14	14	-1	1	27.5000	27.5000	46.8179	100.0
15	15	15	0	1	27.5000	27.5000	30.0000	99.0

Table 5 Second Part of the Domain with CCD for Non-Maneuvering Case

↓	C1	C2	C3	C4	C5	C6	C7	C8
	StdOrder	RunOrder	PtType	Blocks	Altitude (%)	Downrange (%)	LOR (%)	PoH (%)
1	1	1	1	1	15.0000	65.0000	20.0000	62.6
2	2	2	1	1	40.0000	65.0000	20.0000	59.6
3	3	3	1	1	15.0000	90.0000	20.0000	43.8
4	4	4	1	1	40.0000	90.0000	20.0000	37.0
5	5	5	1	1	15.0000	65.0000	40.0000	98.6
6	6	6	1	1	40.0000	65.0000	40.0000	98.8
7	7	7	1	1	15.0000	90.0000	40.0000	93.6
8	8	8	1	1	40.0000	90.0000	40.0000	93.6
9	9	9	-1	1	6.4776	77.5000	30.0000	88.2
10	10	10	-1	1	48.5224	77.5000	30.0000	80.0
11	11	11	-1	1	27.5000	56.4776	30.0000	94.6
12	12	12	-1	1	27.5000	98.5224	30.0000	75.8
13	13	13	-1	1	27.5000	77.5000	13.1821	19.2
14	14	14	-1	1	27.5000	77.5000	46.8179	99.6
15	15	15	0	1	27.5000	77.5000	30.0000	84.4

Two different second-order mathematical models are generated with Minitab that represents the effect of the selected factors on the responses as seen below for each of the low downrange and high downrange domains. Naturally, these second-order models involve the main effects, interaction effects and also the curvatures, as previously mentioned.

$$\begin{aligned}
 y_1 = & 37.8104 - 1.0329 \times \text{alt} - 1.7168 \times \text{down} \\
 & + 5.6287 \times \text{LOR} + 0.0045 \times \text{alt}^2 \\
 & + 0.0036 \times \text{down}^2 - 0.0961 \times \text{LOR}^2 \\
 & + 0.0075 \times \text{alt} \times \text{down} \\
 & + 0.0154 \times \text{alt} \times \text{LOR} \\
 & + 0.0354 \times \text{down} \times \text{LOR}
 \end{aligned}$$

$$\begin{aligned}
 y_2 = & 29.8134 + 0.0621 \times \text{alt} - 1.0134 \times \text{down} \\
 & + 5.2946 \times \text{LOR} - 0.0046 \times \text{alt}^2 \\
 & - 0.0021 \times \text{down}^2 - 0.0945 \times \text{LOR}^2 \\
 & - 0.0032 \times \text{alt} \times \text{down} \\
 & + 0.0100 \times \text{alt} \times \text{LOR} \\
 & + 0.0312 \times \text{down} \times \text{LOR}
 \end{aligned}$$

To find out the adequacy of the model, gained data from Monte-Carlo simulations should satisfy the requirement that data should be distributed as Gaussian. For checking the normality condition, the p-values are considered. For this purpose, the required hypotheses are defined as:

- h_0 : The data is normally distributed
- h_1 : The data is not normally distributed

These analysis results are shown in figures. From these figures it may be observed that the data is normally distributed, and the residuals are distributed randomly, meaning that there is no correlation between the residuals and the factors. It may also be seen in the upper left part of the figures that the related p-value to the normality test is 0.956 and 0.109, respectively. Since p-values are higher than 0.05, which is the predetermined threshold value, the normality test is satisfied and the null hypotheses is failed to reject. In addition, the distribution of the fitted values is presented in the upper right corner of these figures. In the lower left part of the figures, frequency of the residuals, and at the lower right hand side. The residuals with respect to the simulation run number may be observed. These results show that the response surfaces constructed are quite sufficient, and normally distributed.

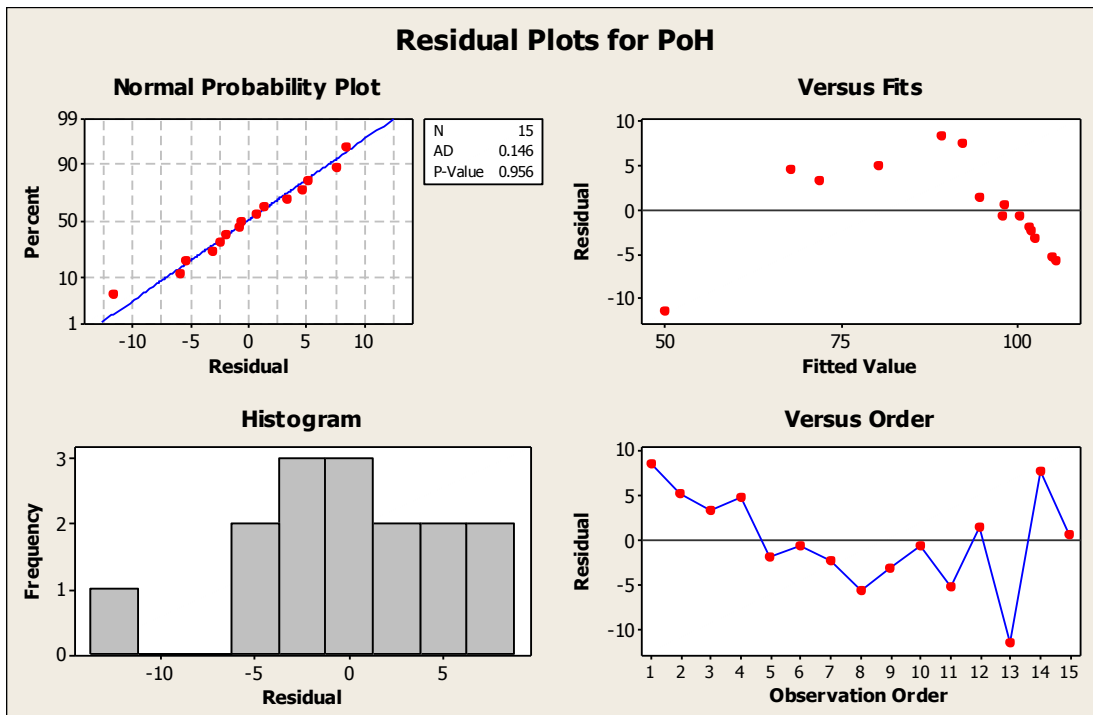


Figure 22 Residual Plots for PoH for Non-Maneuvering Case regarding to first part

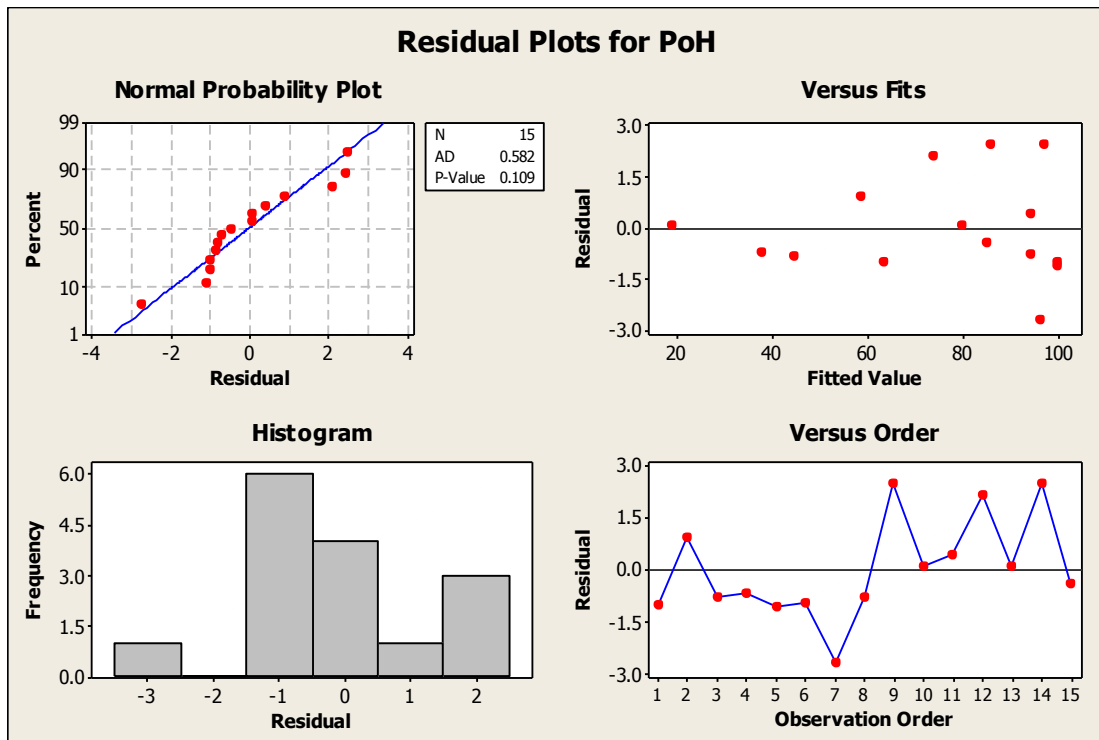


Figure 23 Residual Plots for PoH for Non-Maneuvering Case regarding to second part

Mathematical models can be used for representing the whole operational area under the predetermined bounds. The PoH values may now be obtained using the models developed. These values are graphically shown in figures, for three different LOR values. Comparing these results with the full grid analysis results indicate that the PoH values obtained from the 2nd order RSM's are quite close to those obtained from normal grid analysis.

Finally, it should be noted that these results are obtained from

$$\begin{aligned}
 &2 \times 15 \text{ (number of first RSM area points)} \\
 &= 30 \text{ Monte - Carlo runs} \\
 &30 \times 500 = 15,000 \text{ simulations}
 \end{aligned}$$

Then the number of simulations becomes $30 \times 500 = 15,000$ with respective R-square values of 90% for low-range RSM, and 99.7% for high-range RSM, and with corresponding σ -values of 9.07 and 2.47, respectively.

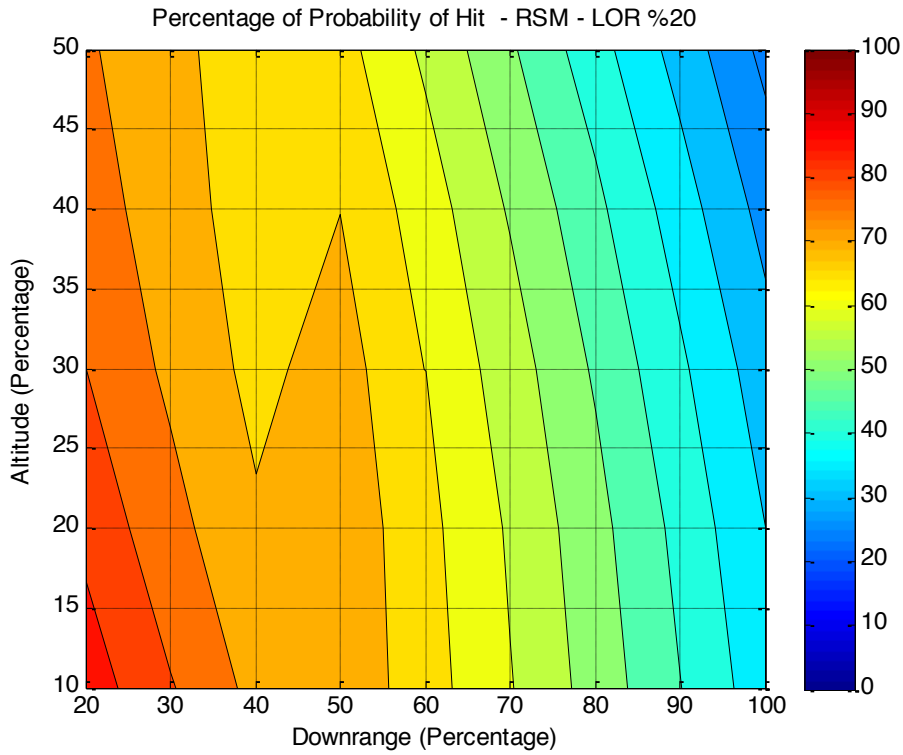


Figure 24 PoH Results for RSM approach for Non-Maneuvering Case at LOR %20

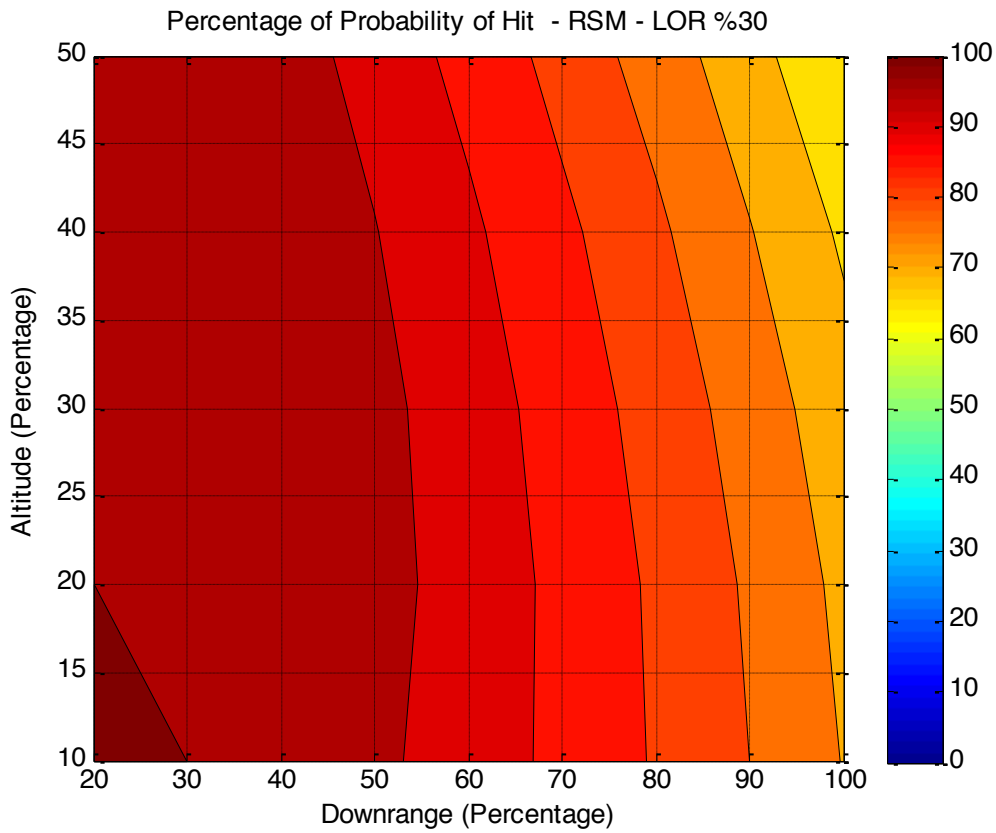


Figure 25 PoH Results for RSM approach for Non-Maneuvering Case at LOR %30

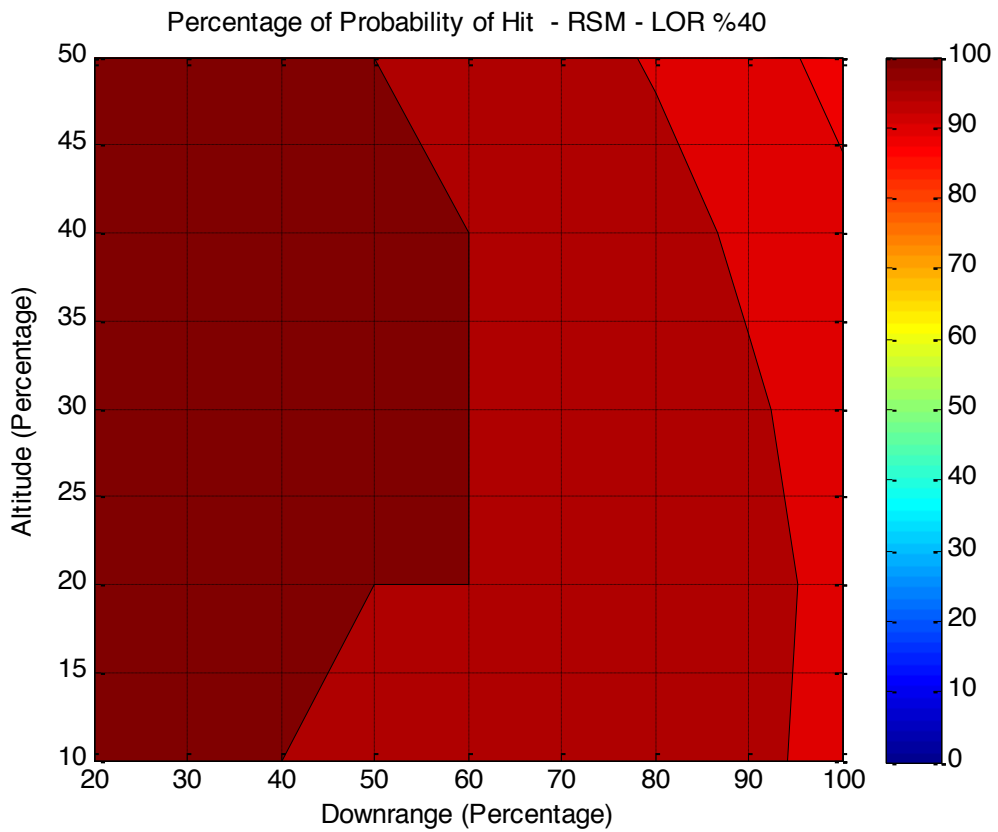


Figure 26 PoH Results for RSM approach for Non-Maneuvering Case at LOR %40

4.3.2 RSM Approach for Maneuvering Cases

Two central composite sample point designs are made with same factors but different values. The necessary minimum and maximum values of the selected factors, determined by Minitab, are chosen in such a way that they contain the whole parameter value space as the ones like in normal grid analysis.

4.3.2.1 RSM Approach for Maneuvering Start-up Range %12

The required parameter combinations, given in the tables, are generated by Minitab:

Table 6 First Part of the Domain with CCD for Maneuvering Startup Range %12

↓	C1	C2	C3	C4	C5	C6	C7	C8
	StdOrder	RunOrder	PtType	Blocks	Altitude (%)	Downrange (%)	LOR (%)	PoH (%)
1	1	1	1	1	12.0000	32.5000	12.0000	90.8
2	2	2	1	1	24.0000	32.5000	12.0000	88.2
3	3	3	1	1	12.0000	49.5000	12.0000	77.8
4	4	4	1	1	24.0000	49.5000	12.0000	66.0
5	5	5	1	1	12.0000	32.5000	24.0000	100.0
6	6	6	1	1	24.0000	32.5000	24.0000	100.0
7	7	7	1	1	12.0000	49.5000	24.0000	100.0
8	8	8	1	1	24.0000	49.5000	24.0000	99.6
9	9	9	-1	1	7.9092	41.0000	18.0000	99.4
10	10	10	-1	1	28.0908	41.0000	18.0000	97.6
11	11	11	-1	1	18.0000	26.7048	18.0000	99.4
12	12	12	-1	1	18.0000	55.2952	18.0000	95.8
13	13	13	-1	1	18.0000	41.0000	7.9092	44.2
14	14	14	-1	1	18.0000	41.0000	28.0908	100.0
15	15	15	0	1	18.0000	41.0000	18.0000	99.2

Table 7 Second Part of the Domain with CCD for Maneuvering Startup Range %12

↓	C1	C2	C3	C4	C5	C6	C7	C8
	StdOrder	RunOrder	PtType	Blocks	Altitude (%)	Downrange (%)	LOR (%)	PoH (%)
1	1	1	1	1	12.0000	75.0000	12.0000	59.8
2	2	2	1	1	24.0000	75.0000	12.0000	38.6
3	3	3	1	1	12.0000	92.0000	12.0000	15.6
4	4	4	1	1	24.0000	92.0000	12.0000	1.0
5	5	5	1	1	12.0000	75.0000	24.0000	99.2
6	6	6	1	1	24.0000	75.0000	24.0000	90.2
7	7	7	1	1	12.0000	92.0000	24.0000	57.2
8	8	8	1	1	24.0000	92.0000	24.0000	8.8
9	9	9	-1	1	7.9092	83.5000	18.0000	85.0
10	10	10	-1	1	28.0908	83.5000	18.0000	10.4
11	11	11	-1	1	18.0000	69.2048	18.0000	92.2
12	12	12	-1	1	18.0000	97.7952	18.0000	3.8
13	13	13	-1	1	18.0000	83.5000	7.9092	7.2
14	14	14	-1	1	18.0000	83.5000	28.0908	86.8
15	15	15	0	1	18.0000	83.5000	18.0000	61.0

Two different second-order mathematical models are generated with Minitab that represents the effect of the selected factors on the responses as seen below for each of the low downrange and high downrange domains. Naturally, these second-order models involve the main effects, interaction effects and also the curvatures, as previously mentioned.

$$\begin{aligned}
 y1 = & 56.142 - 0.277x - 1.279y + 6.895z \\
 & + 0.004x^2 - 0.002y^2 - 0.255z^2 \\
 & - 0.024xy + 0.049xz + 0.085yz
 \end{aligned}$$

$$\begin{aligned}
 y2 = & -539.106 + 10.216x + 11.135y + 18.281z \\
 & - 0.134x^2 - 0.065y^2 - 0.141z^2 \\
 & - 0.080xy - 0.075xz - 0.102yz
 \end{aligned}$$

To find out the adequacy of the model, gained data from Monte-Carlo simulations should satisfy the requirement that data should be distributed as Gaussian. For checking the normality condition, the p-values are considered. For this purpose, the required hypotheses are defined as:

- h_0 : The data is normally distributed
- h_1 : The data is not normally distributed

From the figures it may be observed that the data is normally distributed, and the residuals are distributed randomly, meaning that there is no correlation between the residuals and the factors, as same as the non-maneuvering case. From the upper left part of the figures it can be seen that the related p-value to the normality test is 0.78 and 0.953, respectively. In addition, because p-values are higher than 0.05, which is the predetermined threshold value, the normality test is satisfied and the null hypotheses is failed to reject. The results show that the response surfaces constructed are quite sufficient, and normally distributed.

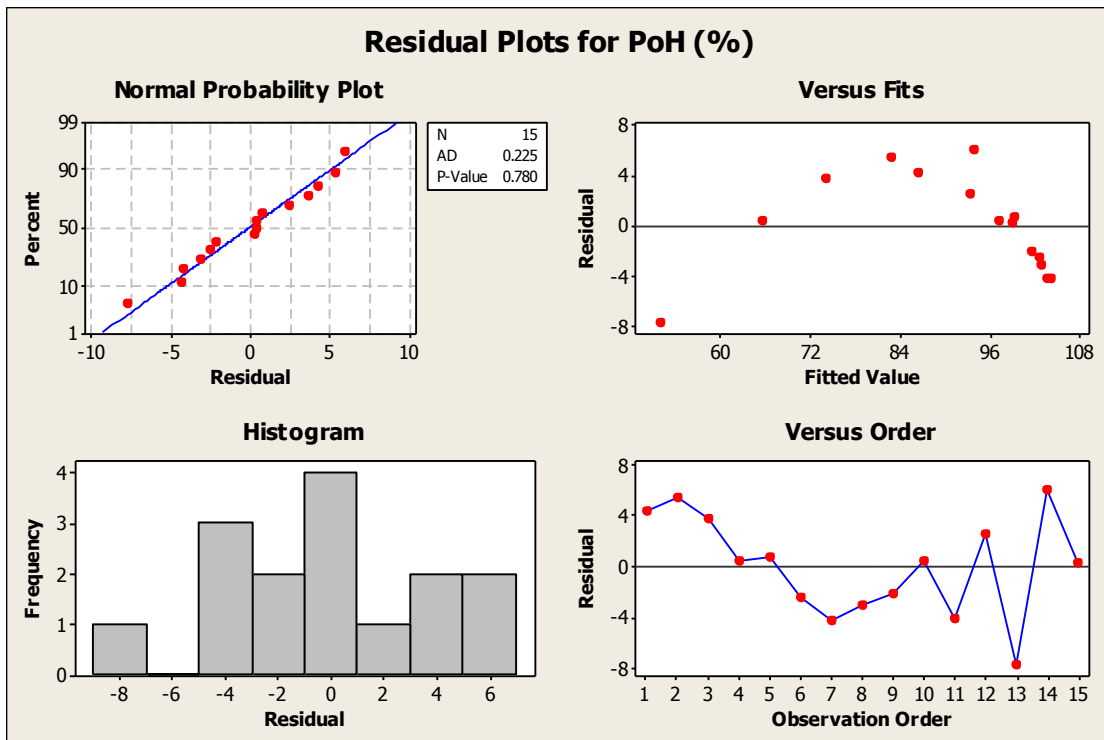


Figure 27 Residual Plots for PoH for Maneuver Start-up range %12 regarding to first part

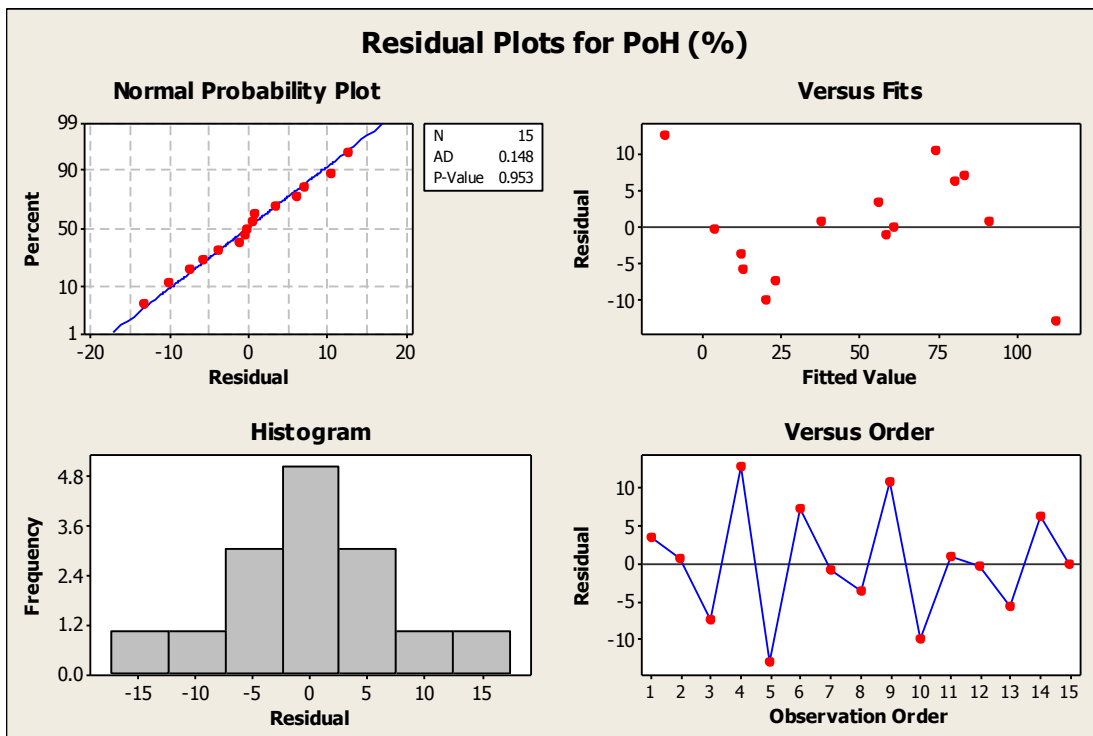


Figure 28 Residual Plots for PoH for Maneuver Start-up range %12 regarding to second part

Mathematical models can be used for representing the whole operational area under the predetermined bounds. The PoH values may now be obtained using the models developed. These values are graphically shown in figures, for three different LOR values. Comparing these results with the full grid analysis results indicate that the PoH values obtained from the 2nd order RSM's are quite close to those obtained from normal grid analysis.

Finally, it should be noted that these results are obtained from $\rightarrow 2 \times 15$ (number of RSM area points) = 30 Monte-Carlo runs. Then the number of simulations becomes $\rightarrow 30 \times 500 = 15,000$ with respective R-square values of

- Low range & Low maneuver $\rightarrow 94\%$
- Low range & High maneuver $\rightarrow 90\%$

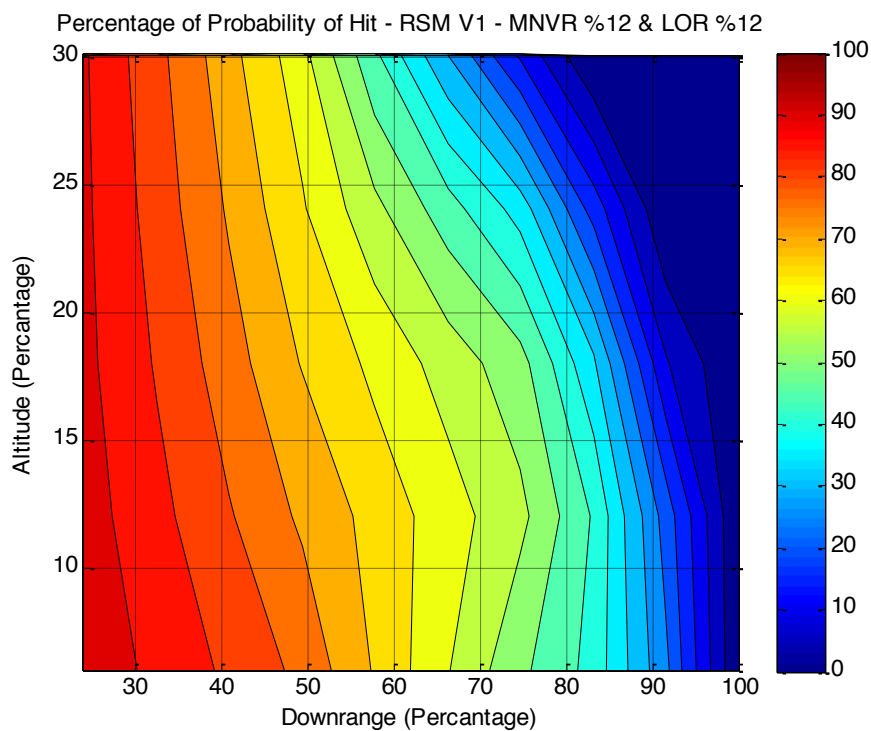


Figure 29 PoH Results for RSM approach for Maneuver Start-up Range %12 at LOR %20

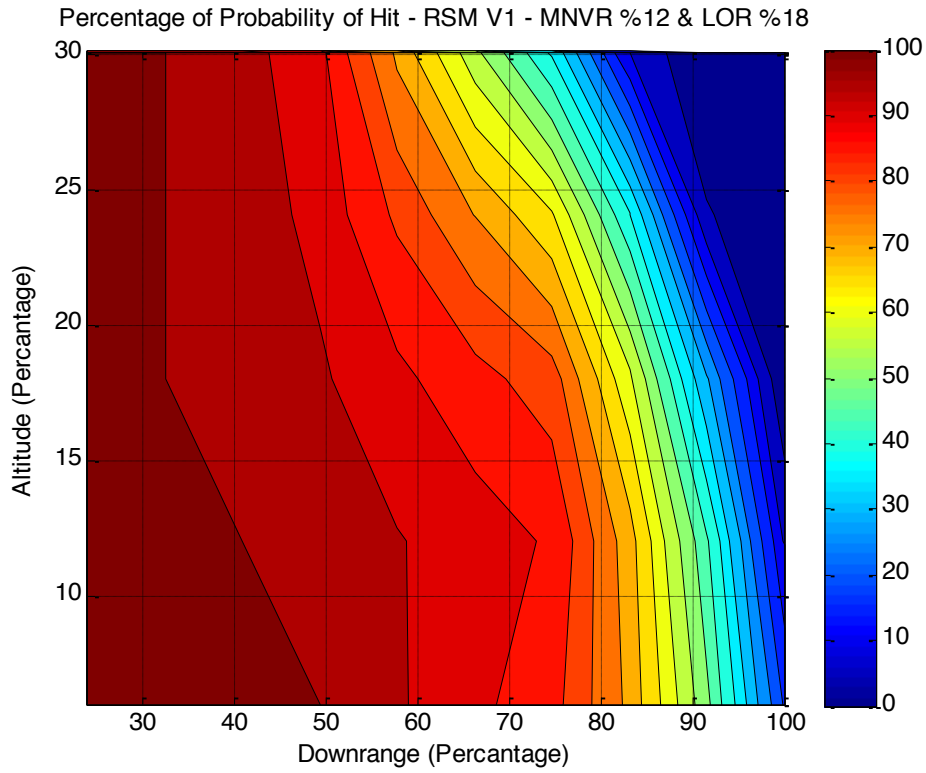


Figure 30 PoH Results for RSM approach for Maneuver Start-up Range %12 at LOR %30

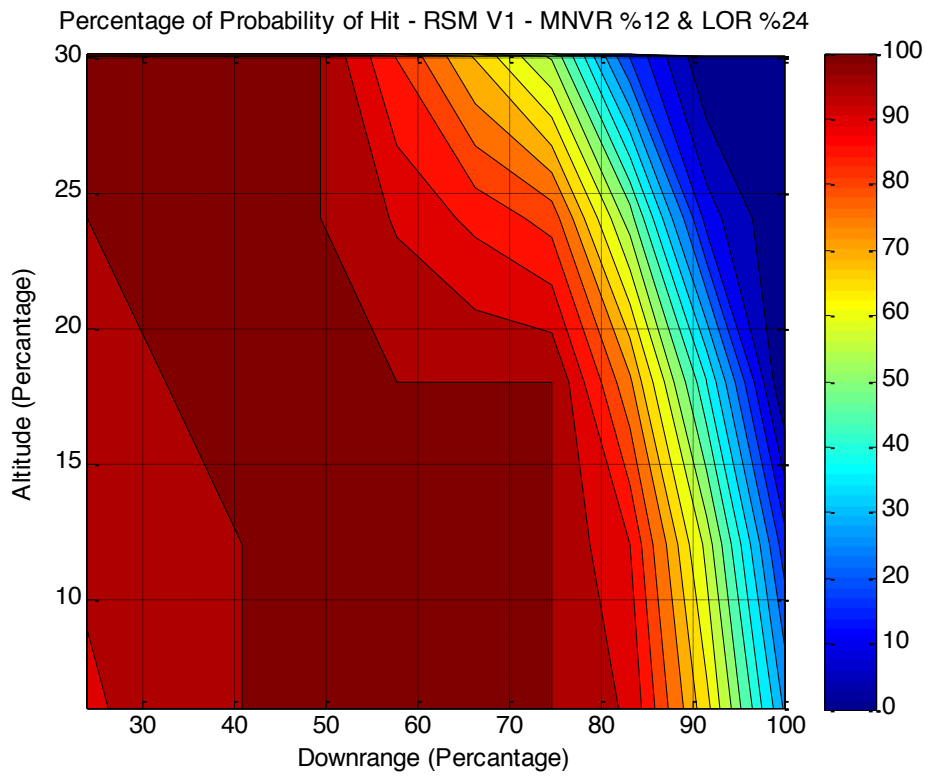


Figure 31 PoH Results for RSM approach for Maneuver Start-up Range %12 at LOR %40

4.3.2.2 RSM Approach for Maneuvering Start-up Range %18

The required parameter combinations, given in the tables, are generated by Minitab:

Table 8 First Part of the Domain with CCD for Maneuvering Startup Range %18

↓	C1	C2	C3	C4	C5	C6	C7	C8	C9	C10
	StdOrder	RunOrder	PtType	Blocks	Altitude (%)	Downrange (%)	LOR (%)	PoH (%)	FITS1	RES11
1	1	1	1	1	12.0000	32.5000	12.0000	86.8	78.949	7.8510
2	2	2	1	1	24.0000	32.5000	12.0000	85.8	75.966	9.8338
3	3	3	1	1	12.0000	49.5000	12.0000	75.8	67.495	8.3046
4	4	4	1	1	24.0000	49.5000	12.0000	63.4	58.713	4.6873
5	5	5	1	1	12.0000	32.5000	24.0000	100.0	100.679	-0.6786
6	6	6	1	1	24.0000	32.5000	24.0000	100.0	104.296	-4.2958
7	7	7	1	1	12.0000	49.5000	24.0000	100.0	105.825	-5.8250
8	8	8	1	1	24.0000	49.5000	24.0000	99.8	103.642	-3.8423
9	9	9	-1	1	7.9092	41.0000	18.0000	99.8	103.606	-3.8065
10	10	10	-1	1	28.0908	41.0000	18.0000	97.4	99.263	-1.8628
11	11	11	-1	1	18.0000	26.7048	18.0000	99.4	105.025	-5.6250
12	12	12	-1	1	18.0000	55.2952	18.0000	94.8	94.844	-0.0442
13	13	13	-1	1	18.0000	41.0000	7.9092	17.0	33.308	-16.3079
14	14	14	-1	1	18.0000	41.0000	28.0908	100.0	89.361	10.6386
15	15	15	0	1	18.0000	41.0000	18.0000	98.8	97.827	0.9727

Table 9 Second Part of the Domain with CCD for Maneuvering Startup Range %18

↓	C1	C2	C3	C4	C5	C6	C7	C8	C9	C10
	StdOrder	RunOrder	PtType	Blocks	Altitude (%)	Downrange (%)	LOR (%)	PoH (%)	FITS1	RES11
1	1	1	1	1	12.0000	75.0000	12.0000	53.8	54.154	-0.3538
2	2	2	1	1	24.0000	75.0000	12.0000	25.0	21.493	3.5071
3	3	3	1	1	12.0000	92.0000	12.0000	2.8	10.165	-7.3654
4	4	4	1	1	24.0000	92.0000	12.0000	0.0	-6.596	6.5955
5	5	5	1	1	12.0000	75.0000	24.0000	98.8	107.930	-9.1303
6	6	6	1	1	24.0000	75.0000	24.0000	76.0	71.169	4.8306
7	7	7	1	1	12.0000	92.0000	24.0000	17.4	23.442	-6.0418
8	8	8	1	1	24.0000	92.0000	24.0000	0.4	2.581	-2.1810
9	9	9	-1	1	7.9092	83.5000	18.0000	68.8	56.411	12.3892
10	10	10	-1	1	28.0908	83.5000	18.0000	2.6	11.405	-8.8045
11	11	11	-1	1	18.0000	69.2048	18.0000	90.0	90.540	-0.5404
12	12	12	-1	1	18.0000	97.7952	18.0000	0.0	-4.125	4.1251
13	13	13	-1	1	18.0000	83.5000	7.9092	1.0	3.639	-2.6392
14	14	14	-1	1	18.0000	83.5000	28.0908	62.8	56.576	6.2239
15	15	15	0	1	18.0000	83.5000	18.0000	38.4	39.015	-0.6150

Two different second-order mathematical models are generated with Minitab that represents the effect of the selected factors on the responses as seen below for each of the low downrange and high downrange domains. Naturally, these second-order

models involve the main effects, interaction effects and also the curvatures, as previously mentioned.

$$\begin{aligned}y_1 = & 32.921 - 1.150x - 2.155y + 11.518z \\ & + 0.035x^2 + 0.010y^2 - 0.358z^2 \\ & - 0.028xy + 0.046xz + 0.081yz\end{aligned}$$

$$\begin{aligned}y_2 = & 216.399 - 6.4199x - 4.567y + 22.862z \\ & - 0.050x^2 + 0.021y^2 - 0.088z^2 \\ & + 0.078xy - 0.029xz - 0.199yz\end{aligned}$$

To find out the adequacy of the model, gained data from Monte-Carlo simulations should satisfy the requirement that data should be distributed as Gaussian. For checking the normality condition, the p-values are considered. For this purpose, the required hypotheses are defined as:

- h_0 : The data is normally distributed
- h_1 : The data is not normally distributed

From the figures it may be observed that the data is normally distributed, and the residuals are distributed randomly, meaning that there is no correlation between the residuals and the factors, as same as the non-maneuvering case. From the upper left part of the figures it can be seen that the related p-value to the normality test is 0.383 and 0.243, respectively. In addition, because p-values are higher than 0.05, which is the predetermined threshold value, the normality test is satisfied and the null hypotheses is failed to reject. The results show that the response surfaces constructed are quite sufficient, and normally distributed.

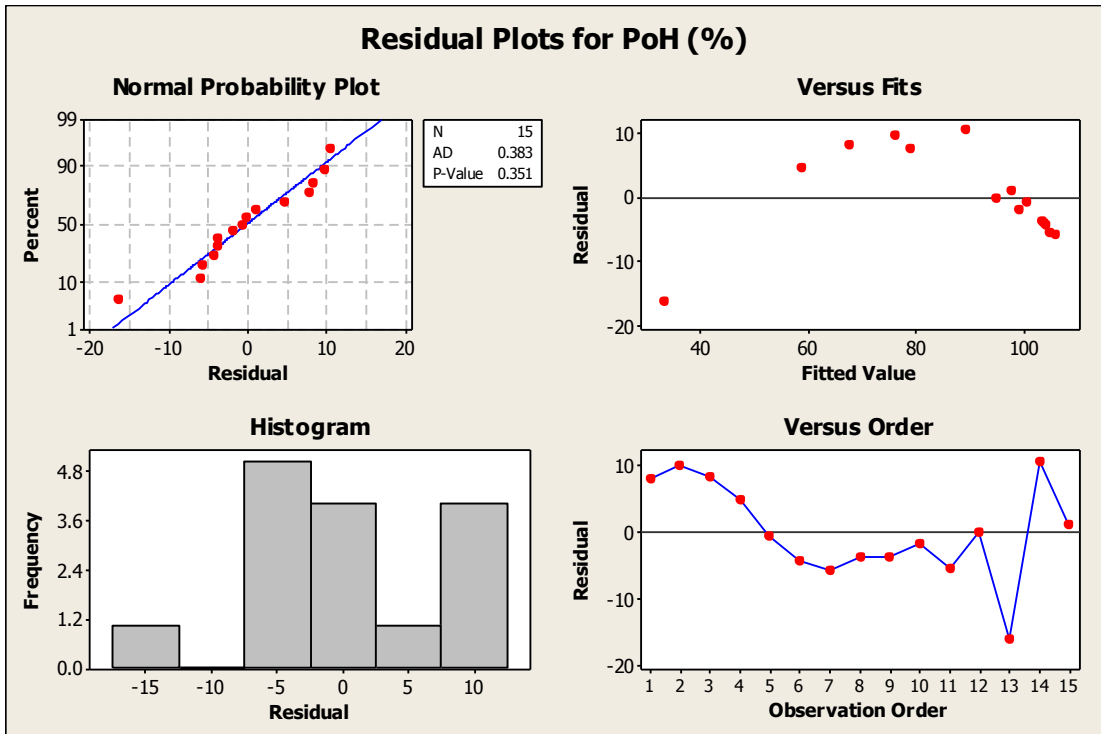


Figure 32 Residual Plots for PoH for Maneuver Start-up range %18 regarding to first part

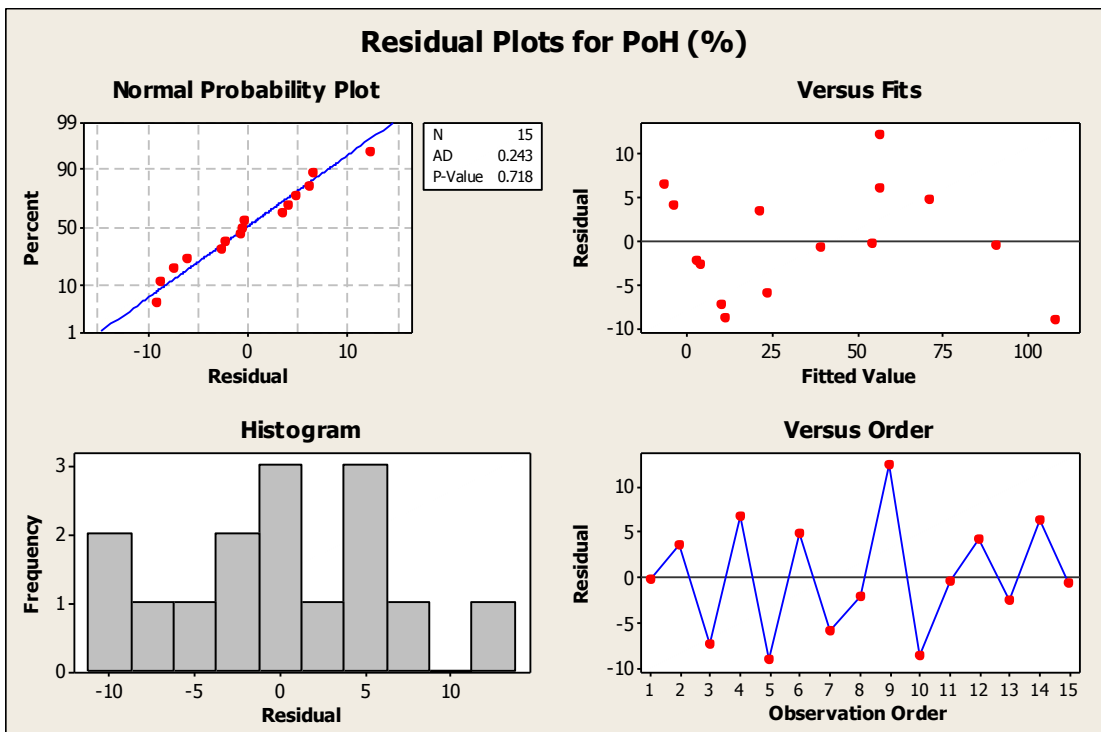


Figure 33 Residual Plots for PoH for Maneuver Start-up range %18 regarding to second part

Mathematical models can be used for representing the whole operational area under the predetermined bounds. The PoH values may now be obtained using the models developed. These values are graphically shown in figures, for three different LOR values. Comparing these results with the full grid analysis results indicate that the PoH values obtained from the 2nd order RSM's are quite close to those obtained from normal grid analysis.

Finally, it should be noted that these results are obtained from $\rightarrow 2 \times 15$ (number of RSM area points) = 30 Monte-Carlo runs. Then the number of simulations becomes $\rightarrow 30 \times 500 = 15,000$ with respective R-square values of

- High range & Low maneuver $\rightarrow 96\%$
- High range & High maneuver $\rightarrow 97\%$

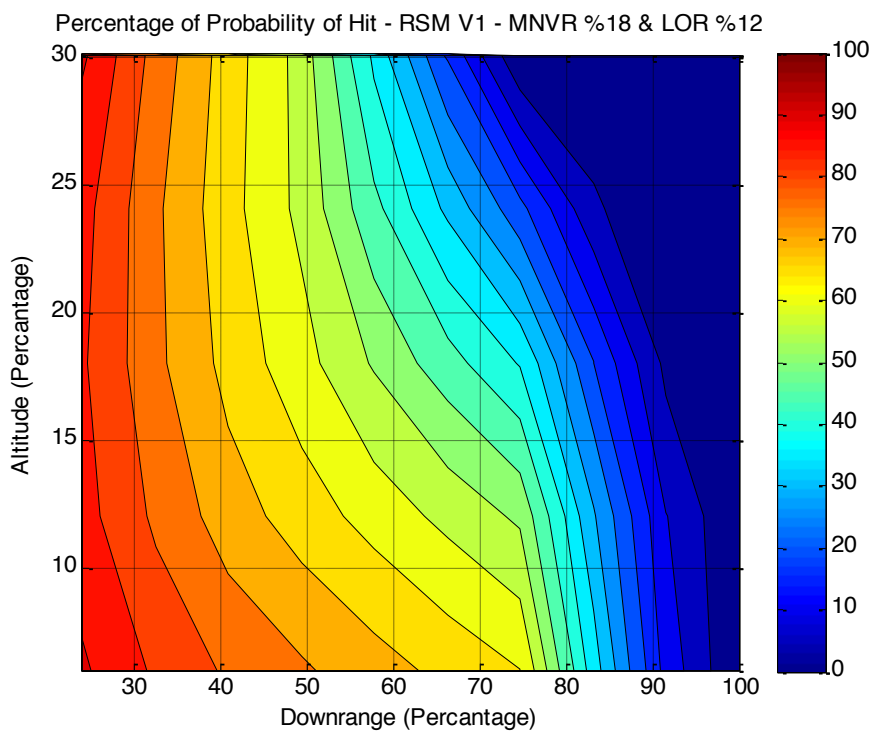


Figure 34 PoH Results for RSM approach for Maneuver Start-up Range %18 at LOR %20

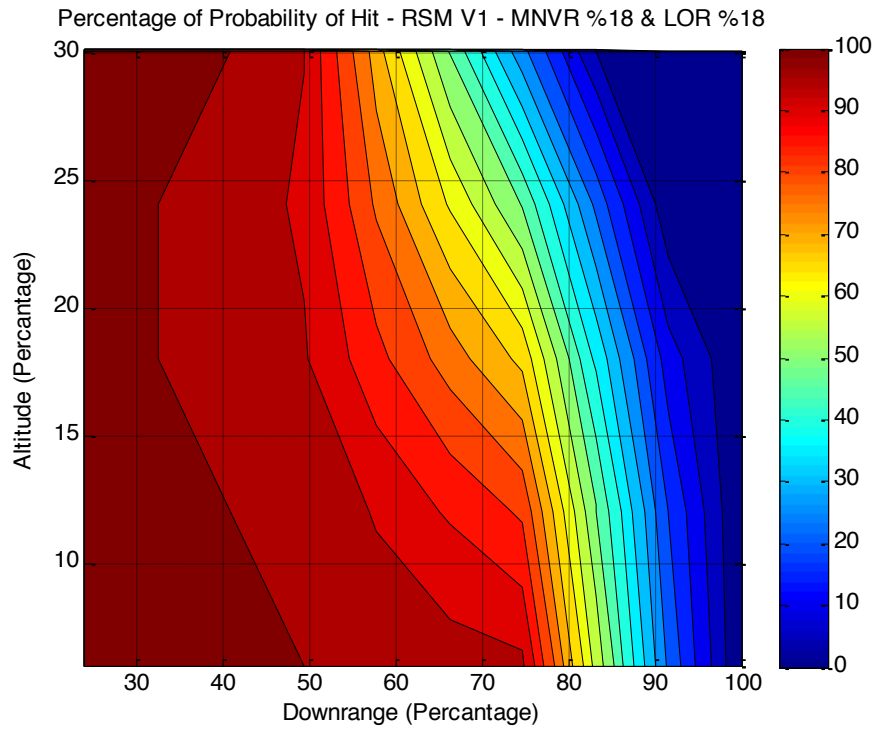


Figure 35 PoH Results for RSM approach for Maneuver Start-up Range %18 at LOR %30

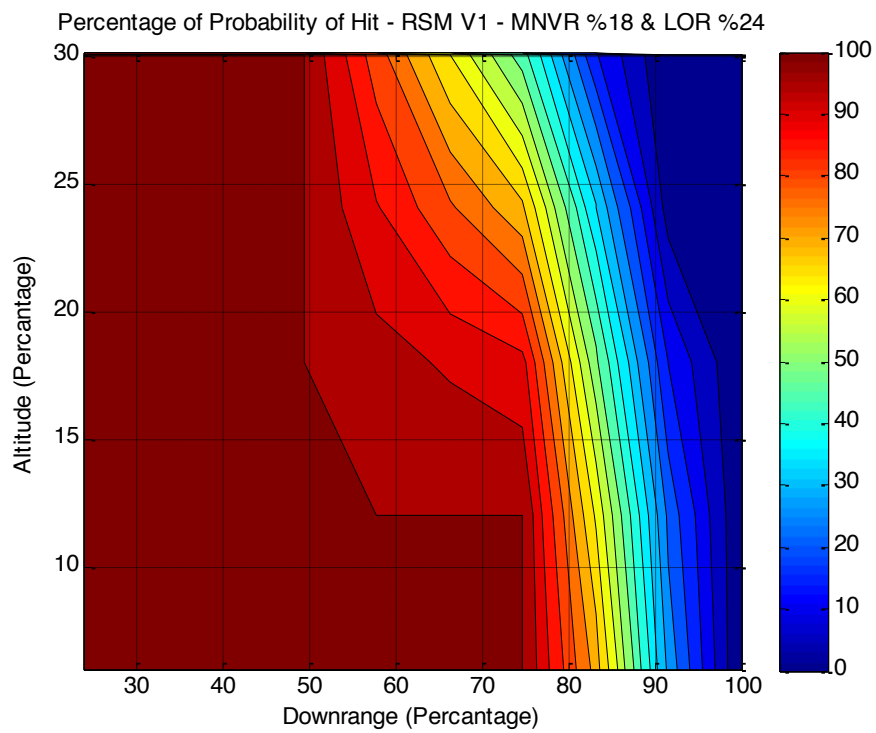


Figure 36 PoH Results for RSM approach for Maneuver Start-up Range %18 at LOR %40

CHAPTER 5

COMPARISON OF GRID AND RESPONSE SURFACE METHODS

In this chapter, in order to see the differences between the results of conventional grid method and response surface methodology, all the graphs are compared to each other. With this way, the effect of the target engagement scenario can also be seen.

5.1 Comparison for Non-Maneuvering Case

The comparison between grid and RSM results for non-maneuvering target can be shown in figures:

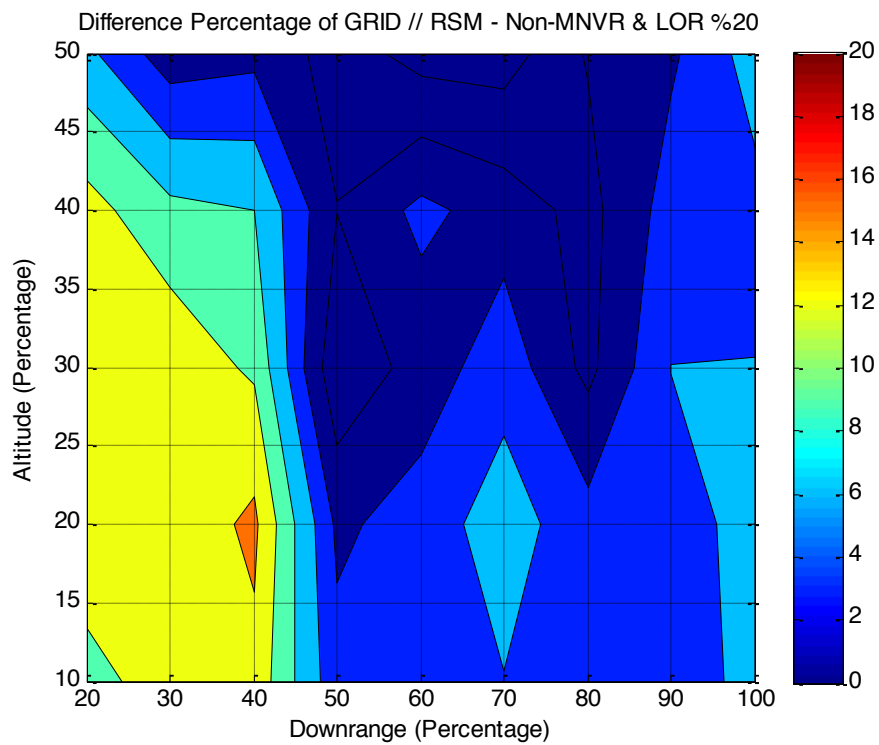


Figure 37 Comparison of PoH Results btw grid and RSM approaches for non-maneuver case LOR %40

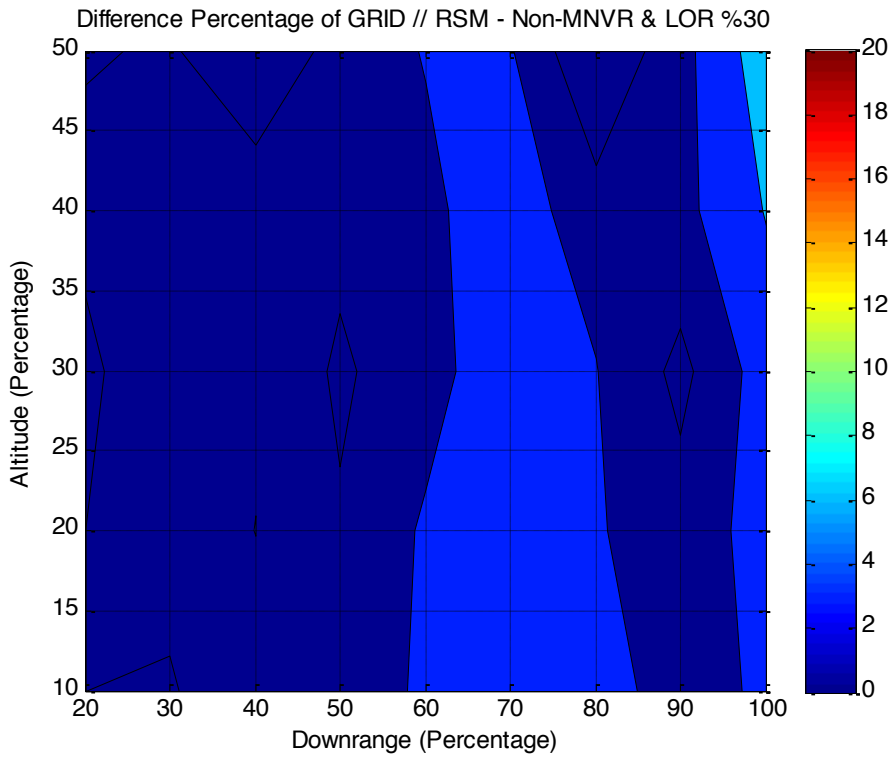


Figure 38 Comparison of PoH Results btw grid and RSM approaches for non-maneuver case LOR %40

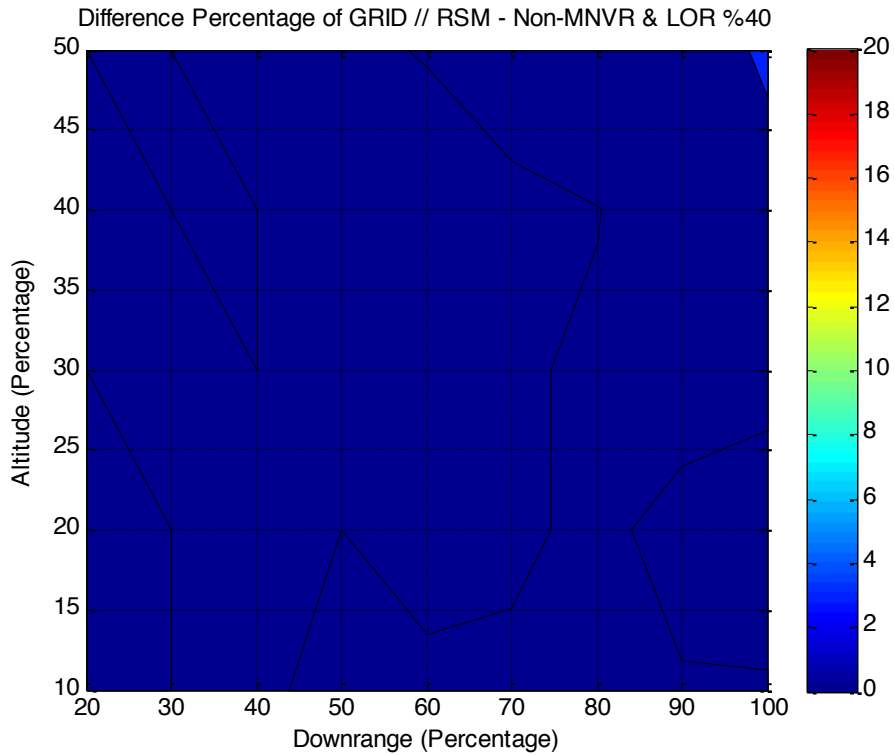


Figure 39 Comparison of PoH Results btw grid and RSM approaches for non-maneuver case LOR %40

It is clear from these figures that, although small, there are some estimation errors between the RSM and grid analyses, especially at the limit conditions of altitude and downrange. This is actually expected since there are no sample points at the boundaries of the regions (Fig. 7). On the other hand, second order RSM results are similar to the improved RSM results for the LOR values of 30% and 40% of the maximum downrange (reference distance). It is clear that improved RSM has less error for the LOR value of 20% of reference distance. In addition, improved RSM analysis has also better goodness-of-fit (R-square) values of 98.8% for part 1 and 99.8% for part 2, and sigma (σ) values of 4.96 for part 1 and 3.01 for part 2.

5.2 Comparison for Maneuvering Start-up Range %12

The comparison between grid and RSM results for maneuvering start-up range %12 can be shown in figures:

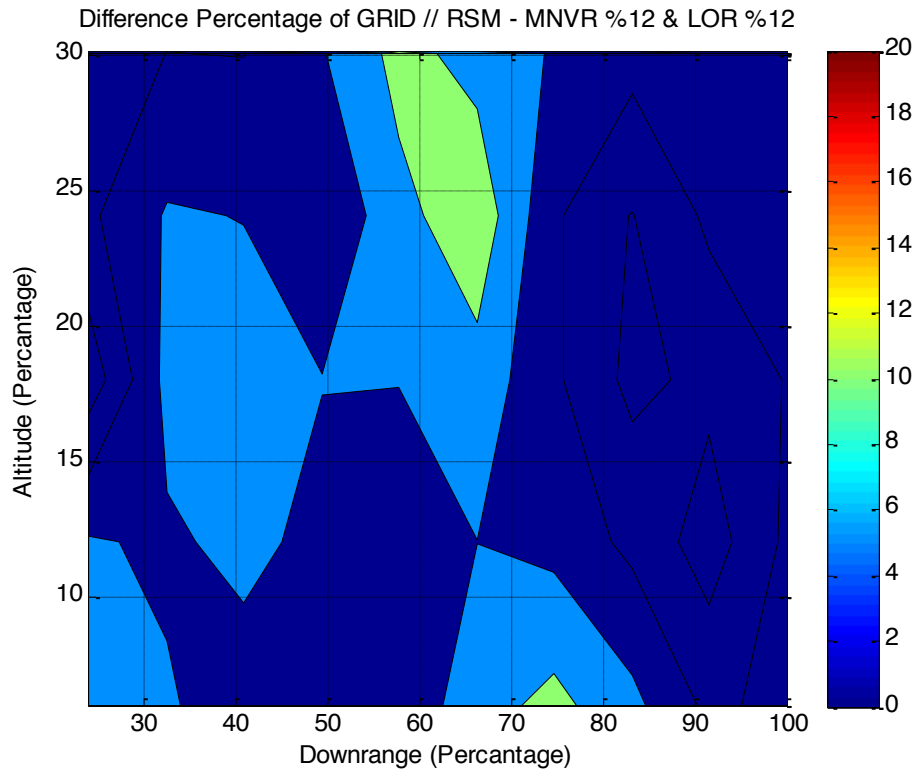


Figure 40 Comparison of PoH Results btw grid and RSM approaches for maneuver start-up range %12 at LOR %12

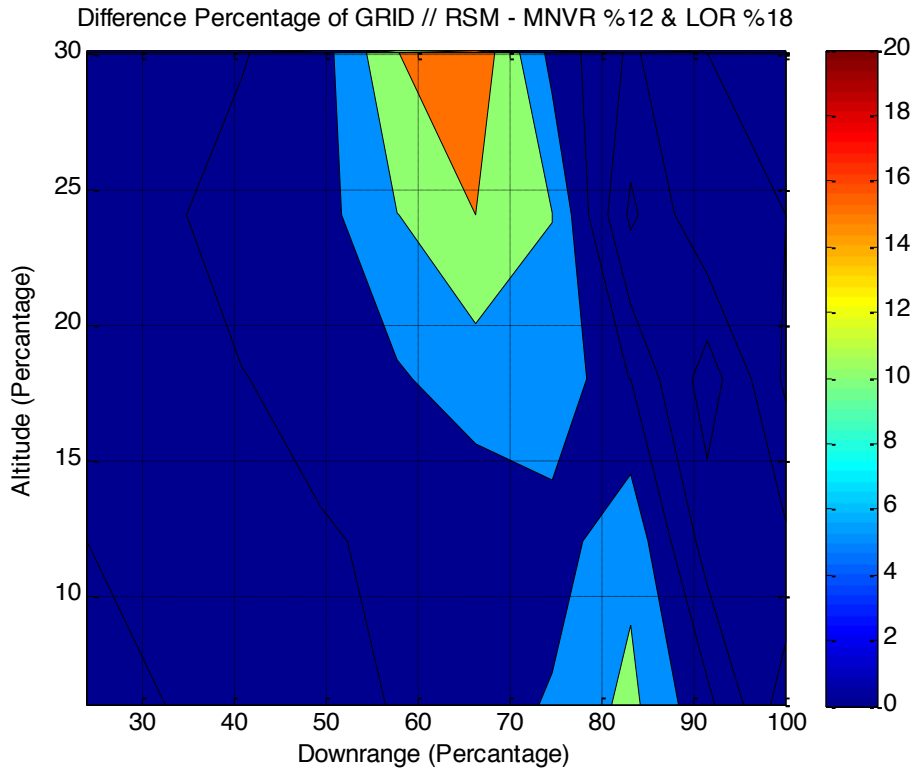


Figure 41 Comparison of PoH Results btw grid and RSM approaches for maneuver start-up range %12 at LOR %18

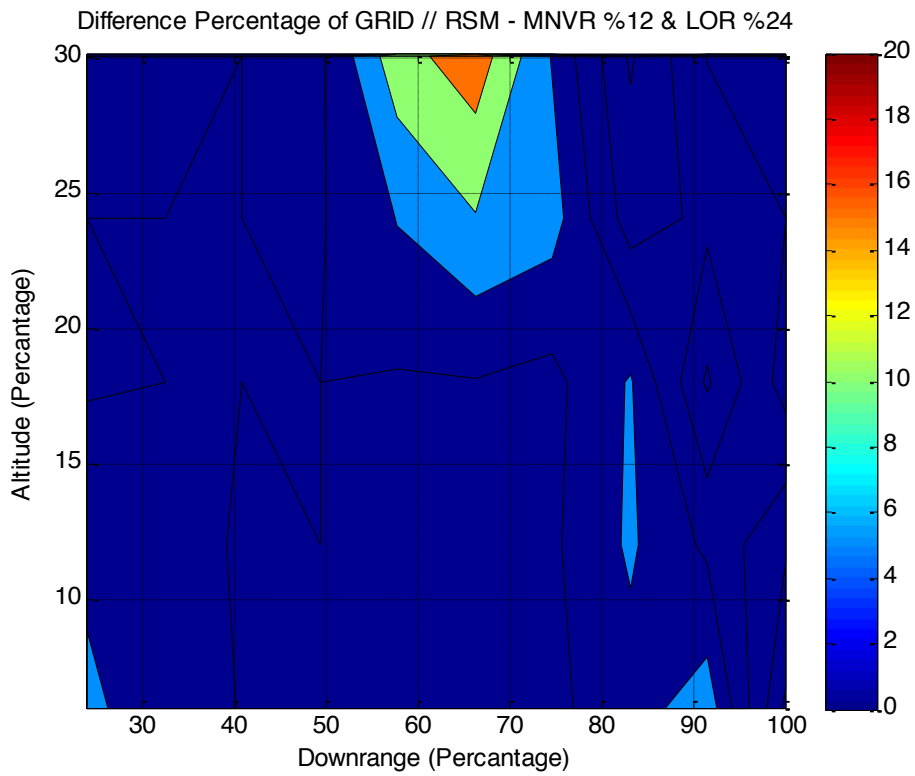


Figure 42 Comparison of PoH Results btw grid and RSM approaches for maneuver start-up range %12 at LOR %24

5.3 Comparison for Maneuvering Start-up Range %18

The comparison between grid and RSM results for maneuvering start-up range %18 can be shown in figures:

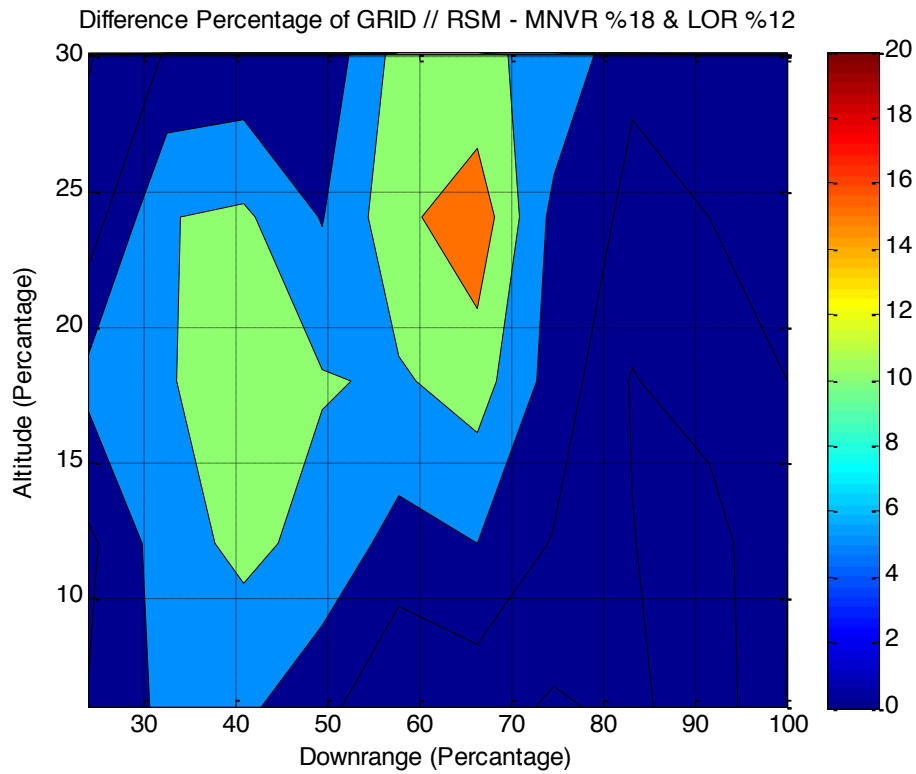


Figure 43 Comparison of PoH Results btw grid and RSM approaches for maneuver start-up range %18 at LOR %12

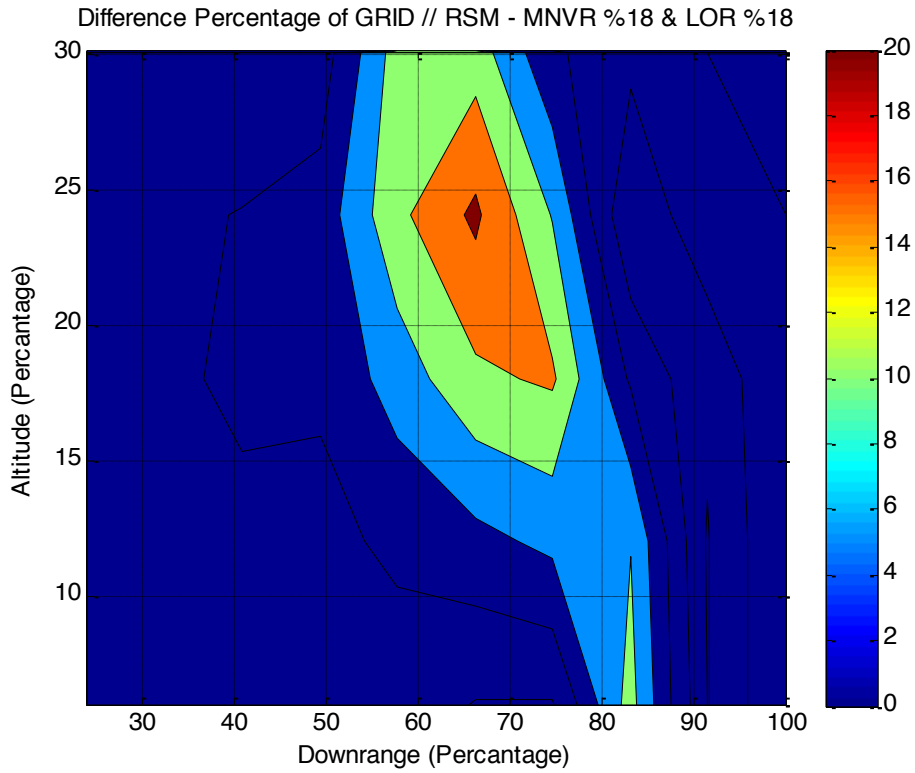


Figure 44 Comparison of PoH Results btw grid and RSM approaches for maneuver start-up range %18 at LOR %18

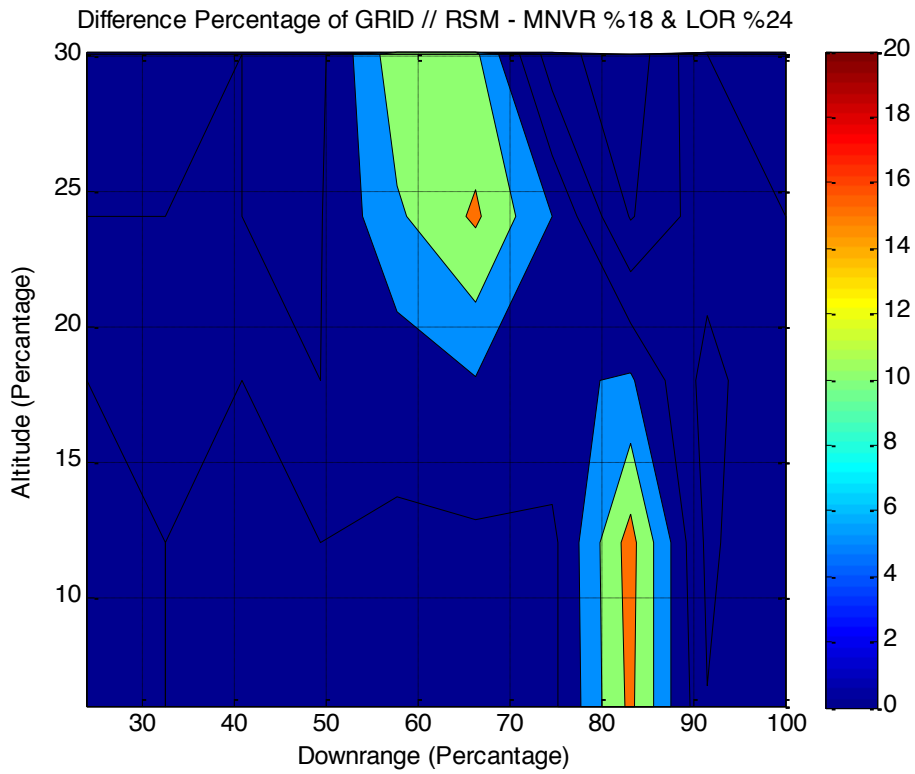


Figure 45 Comparison of PoH Results btw grid and RSM approaches for maneuver start-up range %18 at LOR %24

It is clear from these figures that, although small, there are some estimation errors between the RSM and grid analyses, especially at the limit conditions of altitude and downrange. This is expected since there are no sample points at the boundaries of the regions (Fig. 8). In addition, there are some differences between RSM and GRID methods for the middle range cases, since these points are corresponded to the boundary of the two estimated models. These errors can be avoided by assuming that the engagement treatment does not change dramatically for the middle scenario cases.

CHAPTER 6

CONCLUSION

6.1 General Conclusions

In this thesis, response surface methodology is used to construct the performance prediction model of a missile. The parameter used is the probability of hit.

To demonstrate the idea, a detailed six degrees of freedom missile simulation model is employed. Three target engagement scenario cases are chosen; non-maneuvering and two different maneuvering targets.

The response surfaces obtained are compared to the results of the full grid analysis. The comparisons between the response surface and grid method gives that the error is generally below 5%. Especially for the non-maneuvering case, the results seem much better. In addition, the goodness of fit tests (R-square) is also quite high, more than 90%. This shows that the generated models have good fit for the sampled points. Furthermore, the data collected from the response surface method is convenient for analysis, since it is distributed as normally. To sum up, based on the successful results obtained from the response surface method, the required time for evaluating the performance of an air-defense missile system decreased significantly. For the non-maneuvering cases, since the number of sampling points decreased from 135 to 30, the necessary time for the performance analysis reduced approximately 4.5 times. In a similar manner, the required time for the maneuvering cases decreased approximately five times, since the number of sampling points is decreased from 150 to 30.

6.2 Recommendations for Future Work

The following improvements for the current work are advised:

- ADMS model fidelity may be increased with adding more detailed subsystem models
- Extra response surface analysis areas can be added in order to obtain more accurate results. However, this causes an increasing for the analysis time.
- Additional sample points can be inserted in order to avoid this situation or the system can be modeled with a higher-order polynomial.
- Other statistical design of experiment methods such as krigging and hypercube designs may be used in order to avoid erros occured for not sampled points in the middle ranges.
- Performance analysis may be done for other maneuvere scenarios.

REFERENCES

- [1] Montgomery D.C., *Design and Analysis of Experiments*, New York: Wiley; 2001, Fifth Edition.
- [2] Myers RH, Montgomery D.C., Anderson-Cook C.M., *Response Surface Methodology-Process and Product Optimization Using Designed Experiment*, New York: Wiley; 2009, Third Edition
- [3] Günaydın, K., Çimen, T., and Tekinalp, O., “Response Surface Based Performance Analysis of an Air Defense Missile System,” *Proceedings of the IEEE Aerospace Conference*, Big Sky, MT, 2014.
- [4] Günaydın, K., Çimen, T., and Tekinalp, O., “Response Surface Based Performance Analysis of an Air Defense Missile System Against Maneuvering Targets,” *Proceedings of the AIAA Aviaton Forum 2014 – Modeling and Simulation Technologies*, Atlanta, GA, 2014.
- [5] Khuri A.I., Mukhopadhyay S., *Response Surface Methodology*, Wires Computational Statistics Advanced Review, April 2010
- [6] Bradley N., *the Response Surface Methodology*, Master of Science in Applied Mathematics & Computer Science in Indiana University South Bend, 2007
- [7] Tai J., C., Mavris D., N., Schrage D., P., “Application of a Response Surface Method to the Design of Tipjet Driven Stopped Rotor/Wing Concepts,” *1st AIAA Aircraft Engineerig, Technology, and Operations Congress*, September 1995
- [8] Sevant N.E., Bloor M.I.G., Wilson M.J., “Aerodynamic Design of A Flying Wing Using Response Surface Methodology,” *Journal of Aircraft*, Vol. 37 No.4, July-August 2000
- [9] Englund W.C., Stanley D.O., Lepsch R.A., Mcmillan M.A., Unal R., “Aerodynamic Configuration Design Using Response Surface Methodology Analysis,” *Proceedings of the Aircraft Design, Systems and Operations Meeting*, August 1993

- [10] Colonna M.R., Reddy, S., Alonso J.J., “Multi-Fidelity Trajectory Optimization with Response Surface-Based Aerodynamic Prediction,” *Proceedings of the AIAA Aerospace Sciences Meeting & Exhibit*, January 2008
- [11] Kim Y., Kim J., Jeon Y., Bang J, Lee D.H., Kim Y., Park C., “Multidisciplinary Aerodynamic-Structural Design Optimization Of Supersonic Fighter Wing Using Response Surface Methodology,” *Proceedings of the AIAA Aerospace Sciences Meeting & Exhibit, January 2002*
- [12] Wachter R., Cordery A., “Response Surface Methodology Modelling of Diamond-Like Carbon Film Decomposition,” *Current UK Research in Carbon Science and Technology*, 1997
- [13] Raux W.J, Stander N., Haftka R.T., “*Response Surface Approximations for Structural Optimization*,” *Proceedings of the AIAA/NASA/ISMI Symposium on Multidisciplinary Analysis and Optimization*, 1996
- [14] Agarwal H., Renaud J.E., “Reliability Based Design Optimization for Multidisciplinary Systems Using Response Surfaces,” *Proceedings of the AIAA/ASME/ASCE/AHS/ASC Structures, Structural Dynamics and Materials Conference*, April 2002
- [15] Joyner C., Sabatella J., “Launch Vehicle Propulsion Optimization Using Response Surface Methodology,” *Proceedings of the AIAA/SAE/ASME/ASEE 26th Joint Propulsion Conference*, 1990
- [16] Vaidyanathan R., Papila N., Shyy W., Tucker P.K., Griffin L.W., Haftka R.T., Fitz-Coy N., “Neural Network and Response Surface Methodology for Rocket Engine Component Optimization,” *Proceedings of the AIAA/USAF/NASA/ISSMO Symposium on Multidisciplinary Analysis and Optimization*, September 2000
- [17] Queipo N.V., Haftka R.T, Shyy W., Goel T., Vaidyanathan R., Tucker P.K., “Surrogate-Based Analysis and Optimization,” *Progress in Aerospace Sciences*,” 2005
- [18] Venter G, Haftka R.T., *Constructions of Response Surface Approximations for Design Optimization*, AIAA Journal, Vol.36 No.12, December 1998

- [19] Koch P.N., Mavris D., Mistree F., “Partitioned, Multilevel Response Surfaces for Modeling Complex Systems,” *AIAA Journal*, Vol. 38 No. 5, May 2000
- [20] Venter G, Haftka R.T., Starnets H.S.Jr., “Construction of Response Surfaces for Design Optimization Applications,” *Proceedings of the AIAA/NASA/ISMO Symposium on Multidisciplinary Analysis and Optimization*, 1996
- [21] Li G., Grandhi R., “Accuracy and Efficiency Improvement of Response Surface Methodology for Multidisciplinary Design and Optimization,” *Proceedings of the AIAA/USAF/NASA/ISSMO Symposium on Multidisciplinary Analysis and Optimization*, September 2000
- [22] https://wiki.ece.cmu.edu/ddl/index.php/Experimental_design [last accessed on 25.08.2014]
- [23] Taguchi G., Yokoyama Y., Wu Y., “*Taguchi Methods: Design and Experiments*,” American Supplier Institute, 1993
- [24] https://controls.engin.umich.edu/wiki/index.php/Design_of_experiments_via_taguchi_methods:_orthogonal_arrays [last accessed on 25.08.2014]
- [25] <http://www.allpm.com/index.php/about/item/419-elements-and-components-of-a-doe-the-fundamentals-of-design-of-experiments-part-ii-of-iii-by-harry-rever-pmp-ndash-director-of-six-sigma-iil> [last accessed on 25.08.2014]
- [26] <http://www.opexresources.com/index.php/free-resources/articles/analysis-of-residuals-explained> [last accessed on 25.08.2014]
- [27] http://isd.kjist.ac.kr/optimization/optimization_upper.htm [last accessed on 25.08.2014]
- [28] MATLAB/Simulink (R2009a), The Mathworks Inc., 2009
- [29] Minitab 16.2.2, Minitab Inc., 2010